

TNO Defence Research

TD 93-3418

Phone +31 70 326 42 21

TNO-report
FEL-93-A323

copy nr
8

title
Evaluation of FEL image processing algorithm for 12-bit
CCD-images as function of various atmospheric conditions

0

AD-A285 187



DISTRIBUTION STATEMENT A

Approved for public release
Distribution Unlimited

OTIC
LECTE
OCT 04 1994
S B D

TDCK RAPPORTENCENTRALE

Frederikkazerne, gebouw 140
v/d Burchlaan 31 MPC 16A
TEL. : 070-3166394/6395
FAX. : (31) 070-3166202
Postbus 90701
2509 LS Den Haag

TD 93-3418

TNO Defence Research

TNO
Lab **TD 93-3418**
Oude Waalsdorperweg 63
2597 AK The Hague
P.O. Box 96864
2509 JG The Hague
The Netherlands
Fax +31 70 328 09 61
Phone +31 70 326 42 21

TNO-report
FEL-93-A323

copy nr.
8

title
Evaluation of FEL image processing algorithm for 12-bit
CCD-images as function of various atmospheric conditions

author(s):

J.A. Boden

TDCK RAPPORTCENTRALE
Frederikkazerne, gebouw 140
v/d Burchlaan 31 **MPC 16A**
TEL. : 070-3166394/6395
FAX. : (31) 070-3166202
Postbus 90701
2509 LS Den Haag **TDCK**

date:

February 1994

classification

classified by : G. Zwiep

classification date : January 7, 1994

title : ongerubriceerd

managementuitreksel : ongerubriceerd

abstract : ongerubriceerd

report text : ongerubriceerd

appendix A : ongerubriceerd

94-31562


All rights reserved.
No part of this publication may be reproduced and/or published by print, photoprint, microfilm or any other means without the previous written consent of TNO.

In case this report was drafted on instructions, the rights and obligations of contracting parties are subject to either the 'Standard Conditions for Research Instructions given to TNO', or the relevant agreement concluded between the contracting parties.

Submitting the report for inspection to parties who have a direct interest is permitted.

© TNO

no. of copies : 27

no. of pages : 53 (including appendix,
excluding RDP and distribution list)

no of appendices : 1

ONGERUBRICEERD

All information which is classified according to Dutch regulations shall be treated by the recipient in the same way as classified information of corresponding value in his own country. No part of this information will be disclosed to any party.

The classification designation ONGERUBRICEERD is equivalent to UNCLASSIFIED.

Netherlands organization for applied scientific research

TNO Defence Research consists of:
the TNO Physics and Electronics Laboratory,
the TNO Prins Maurits Laboratory and the
TNO Institute for Perception



The Standard Conditions for Research Instructions given to TNO, as filed at the Registry of the District Court and the Chamber of Commerce in The Hague shall apply to all instructions given to TNO.

9410

MANAGEMENTUITTREKSEL

Titel : Evaluatie van het TNO-FEL algoritme voor beeldverbetering met 12-bits
CCD camerabeelden als functie van diverse atmosferische omstandigheden

Auteur(s) : Drs. J.A. Boden

Datum : februari 1994

Opdrachtnr. : A90KL675

IWP-nr. : 715.3

Rapportnr. : FEL-93-A323

Aanleiding en doelstelling van het onderzoek

Door het TNO-FEL is een beeldbewerkingsalgoritme ontwikkeld op basis van adaptieve contrastversterking met het oog op het vergroten van het waarneembereik van camerasystemen onder gevechtsumstandigheden. Het is gebleken dat onder alle omstandigheden beeldbewerking met dit algoritme tot een comfortabeler waarneming en vaak tot een vergroting van het zichtbereik leidt. Onder bepaalde omstandigheden kan het 'zicht' met een faktor 1,5 groter worden, bijvoorbeeld van 4 tot 6 km. Evaluatie van deze bewerking als functie van diverse atmosferische omstandigheden is van groot belang. Deze evaluatie is onderwerp van in dit rapport beschreven studie.

Omschrijving van het onderzoek

Een groot aantal 12-bit beelden zijn zo bewerkt met dit FEL beeldbewerkingsalgoritme dat een optimale presentatie van de door de camera geregistreeerde informatie werd verkregen. De beelden zijn opgenomen met het eerste FEL 12-bit CCD camerasysteem vanaf de toren van het TNO-FEL. De resultaten van de bewerking worden beschreven en toegelicht met een aantal voorbeelden. Verbanden tussen de gevonden beeldbewerkingsparameters en de atmosferische omstandigheden zijn onderzocht. Een duidelijk verband werd gevonden tussen het 'laagste geregistreeerde lichtniveau' in een beeld en de 'relatieve vochtigheid gedeeld door het zicht'. Het algoritme bevat een globale bewerking, de 'stretch' transformatie, en een lokale adaptieve contrastversterking. Bij aanwezigheid van slechts een beperkte lichtomvang (mist, heilig weer), wordt met een 'stretch' transformatie (op de pixelwaarden van het gehele beeld of van een deelbeeld) alleen reeds een aanzienlijke beeldverbetering verkregen.

Conclusies en aanbevelingen

Bij toepassing van het algoritme, vooral bij slecht-zichtsituaties, kunnen meer details via bewerking zichtbaar worden gemaakt en kan dus een vergroting van het zichtbereik gerealiseerd worden. De mate van zichtverbetering hangt, behalve van de camera performance, in de praktijk ook af van de aard van de scene, van aard en mate van het contrastverlies in de atmosfeer en tenslotte ook van de waarnemer. Voor slecht-zichtsituaties (mist en heilig weer) kan een verbetering van het 'zicht' met rond een faktor twee verwacht worden. Een betrouwbare kwantitatieve bepaling vereist zeer geconditioneerde experimenten.

De met deze studie verkregen inzichten zijn benut voor andere CCD projecten. Een 12-bits camerasysteem met PC besturing en met een Peltier gekoelde camerakop werd inmiddels gebouwd om opnamen op willekeurige lokaties te kunnen maken. Hiermee werd bijvoorbeeld een groot aantal opnamen gemaakt tijdens de 'BEST-TWO' battle field trial.

Voor toepassingen is een real time werking van de beeldverbetering van groot belang. Een real time hardware-uitvoering van een variant op het algoritme werd inmiddels gerealiseerd in de vorm van een real time videoprocessor. In het kader van een nationaal technologieproject werd eveneens een real time hardware-uitvoering van het algoritme gerealiseerd tezamen met een aantal real time werkende filtermodules.

De vergroting van herkenningskansen kan op een andere manier afhangen van de bewerking dan de vergroting van het zichtbereik. Onderzoek naar de vergroting van herkenningskansen van diverse militaire objecten, door toepassing van beeldbewerking, wordt aanbevolen. Het is van belang het nut van beeldbewerking verder te kwantificeren en te evalueren onder diverse omstandigheden.

Accession For	
FTIS CRA&I	<input checked="" type="checkbox"/>
DTIC TAB	<input type="checkbox"/>
Unannounced	<input type="checkbox"/>
Justification	
By	
Distribution	
Availability Codes	
Dist	Avail and/or Special
A2	

ABSTRACT

A survey is given of processing results of 12-bit pictures with the FEL image processing algorithm. The results are illustrated with examples. The pictures have been taken with the first FEL 12-bit CCD camera system under various atmospheric conditions. Some relations between processing parameters and atmospheric conditions are analysed. An indication of a quantitative visibility range improvement is given.

SAMENVATTING

De resultaten van de bewerking van 12-bit beelden met het FEL beeldbewerkingsalgoritme worden beschreven en toegelicht met een aantal voorbeelden. De beelden zijn opgenomen onder diverse weersomstandigheden met het eerste FEL 12-bit CCD camera-systeem vanaf de toren van het TNO-FEL.

Enkele relaties tussen beeldbewerkingsparameters en atmosferische omstandigheden zijn onderzocht. Voor de zichtverbetering als resultaat van de beeldbewerking wordt een kwantitatieve indicatie gegeven.

CONTENTS

MANAGEMENTUITTREKSEL	2
ABSTRACT/SAMENVATTING	4
1 INTRODUCTION	7
2 DIGITAL IMAGE PROCESSING	8
2.1 Introduction	8
2.2 The image processing algorithm	8
2.3 Pre processing and Post processing	10
2.3.1 Dark field subtraction	10
2.3.2 Flat field correction	11
2.3.3 Median filtering	12
2.3.4 Histogram modification	12
2.3.5 Correction geometrical distortion	12
3 THE IMAGE DATA BASE	14
3.1 Introduction	14
3.2 Image acquisition	14
3.3 The image database	15
4 VISIBILITY IN THE ATMOSPHERE	18
4.1 Theory	18
5 RESULTS	23
5.1 Evaluation of the image processing	23
5.2 Analysis of the image file.	36
5.3 Visibility range improvement	41
5.4 Processing procedure	43

6	CONCLUSIONS	44
7	EPILOGUE	45
	ACKNOWLEDGEMENT	45
	REFERENCES	46
	APPENDIX A: LIST OF PROCESSED IMAGES AND PROCESSING PARAMETERS	

1 INTRODUCTION

The study to be described in this report is carried out to evaluate a sophisticated TV-perception system based on the first prototype of a 12-bit CCD-camera [1]. The main objectives are: to improve the visibility range and apparently reduce the loss of contrast in the atmosphere. At the Physics and Electronics Laboratory TNO a CCD-camera system has been developed with a 12-bit Intra-scene Dynamic Range. Special attention is paid to the analog electronic read-out circuits and to the cooling of the sensor to obtain the necessary signal-to-noise ratio [1].

To present all the information of a 12-bit image on a monitor, image processing is necessary. A special algorithm has been developed, that transforms the dynamic range of the images to the optimum range of the monitor. Simultaneously the contrasts are enhanced such, that all the recorded information becomes within the perception range. A reduction of the dynamic range also results in a reduction of the contrasts. The digital image processing therefore must do anyhow a contrast enhancement. It is also possible to restore the loss of contrast in the atmosphere with this contrast enhancement.

This report mainly describes the evaluation of the image processing algorithm as function of various atmospheric conditions. In the considered period many pictures have been taken with the TNO-camera system and processed with the algorithm. A data-base of images has been set up and this data-base has been analysed with statistical methods to retrieve possible relationships with meteorological parameters. Also a general parameter setting of the algorithm is determined, such that this set can be applied on images taken under different conditions. This was done in view of possible future automation. A first indication of a quantitative visibility-improvement is given. In chapter two the digital image processing algorithm will be discussed briefly. For a more extended paper on this subject is referred to the report FEL-1988-63 [2] and de Vries [3]. In chapter three a description of the image data-base will be given and the image acquisition will be discussed. A brief introduction to the theory of visibility in the atmosphere will be given in chapter four. It will be shown that carefully defined experiments are necessary to quantify the 'visibility range improvement'. The results will be discussed in chapter five and finally in chapter six some conclusions will be given. This study has been carried out mainly under the assignment number A87/KL/159. A critical analysis of the results and a final update of the report has been carried out under the assignment number A90/KL/675.

2 DIGITAL IMAGE PROCESSING

2.1 Introduction

In this chapter the algorithm used to process the images will be described shortly. For a more extended paper on this subject is referred to the FEL-report FEL-1988-63 [2]. This algorithm for digital image processing has been developed at the Physics and Electronics Laboratory TNO. Also a few pre process and post process procedures will be described. Finally, an optimum procedure for processing the images with the same set of processing parameters will be given.

2.2 The image processing algorithm

The purpose of the image processing is to bring the information recorded with the 12-bit CCD-camera into the perception domain of a monitor. It is necessary therefore, to reduce the dynamic range from 12 bits to 8 bits; it is the common digital input for standard TV applications. This transformation will result in a decrease of contrast. The task of the image processing therefore, is to enhance the small contrasts, which can be due to the loss of contrast in the atmosphere as well due to the dynamic range reduction.

Of course commercially available image processing systems offer a score of relative simple techniques to enhance a digital image. A common disadvantage of these techniques is that often only a part of the image is enhanced at the cost of another part. The here used technique operates on the full image and carries out the enhancement independent of the local brightness.

The range transformation is calculated according the equation <2.1>:

$$Y = k_{out} * X^{\gamma} \quad \langle 2.1 \rangle$$

X is the grey level in the input domain and Y in the output domain.

The technique has the potential of real-time use because each pixel is processed separately and the processing does not require any kind of transform and is not recursive. The dynamic range is transformed in a non-linear way, such that the resulting contrast reduction is independent of the local grey-level.

The equivalent implementation of this transformation is shown in figure 2.1. This implementation has the attractive property that the local difference in the logarithmic domain is equal to the contrast in the input image, so the contrasts can directly be manipulated then.

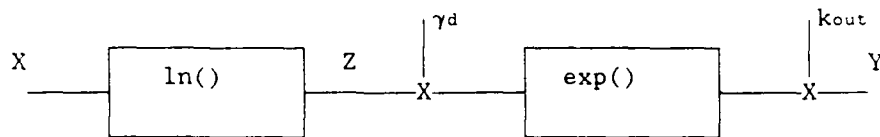


Figure 2.1: The implementation of the dynamic range transformation.

The detail contrast enhancement is carried out by means of a high pass-filtering technique that makes use of only local statistics.

A local difference image is obtained in the logarithmic domain that can be considered as a "contrast image". The local difference image is processed in an adaptive way (the small contrasts are enhanced more than the large ones to prevent artefacts).

An implementation of the filter is shown in figure 2.2.

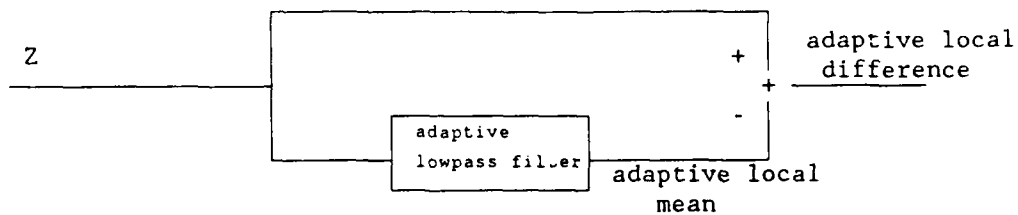


Figure 2.2: The implementation of the filtering technique.

A more extended description of this filter can be found in FEL-report 1988-63 [2]. A combination of the figures 2.1 and 2.2 gives the complete processor, which is shown in figure 2.3.

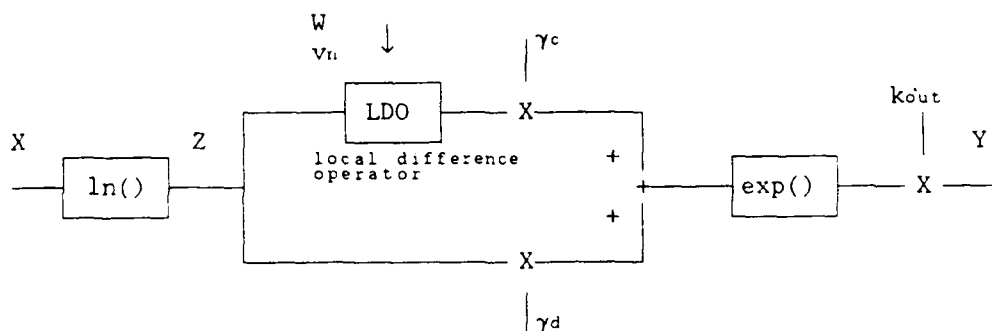


Figure 2.3: A block diagram of the digital image processor. In this diagram W is the filter dimension, v_n is a parameter to adjust the adaptation, γ_c is the contrast parameter and γ_d and k_{out} are the dynamic range reduction parameters.

The optimum value of the adaptation parameter is determined from the local variance range that is present in the image. A threshold value v_n can be defined from that range beyond which the level of contrast enhancement depends on the local variance.

Another advantage of this algorithm is its ability to enhance the high frequencies and to reduce the low frequencies. It means that detail contrast is enhanced, but slowly varying differences in luminance will be eliminated. These variations in luminance can result from the atmosphere or can be due to spatially varying scattering or transmission in the lens and/or the shutter of the camera.

2.3 Pre processing and Post processing

Before images with the above described algorithm are processed, a few preprocessing methods can be applied. Some very common methods will be described here, such as dark field subtraction, flat field correction, median filtering and histogram modification. Post processing eg can be the gamma correction of a TV-monitor and correction of a possible geometrical distortion; this latter eg can arise from differences in the dimensions of the pixels and those of the image section of the CCD-sensor.

2.3.1 Dark field subtraction

Because the effect of the temperature is not uniform across the surface of the CCD, the thermal generation of electrons also is a function of the position. This may cause a noisy picture. By

means of dark field subtraction, which is a very common operation, the rms value of the thermal noise and fixed pattern noise (due to fixed differences in the pixels) can be removed.

The dark field image can be recorded with a closed shutter and with maintaining all the other parameter settings of the camera.

$$\begin{aligned} Y &= 0 && \text{if } X < X_{\text{dark}} \\ Y &= X - X_{\text{dark}} && \text{otherwise} \end{aligned} \quad <2.2>$$

Although the mean level of the thermal noise will be reduced, the standard deviation will increase by a factor $\sqrt{2}$.

Some images have been preprocessed by this method but no clear improvements could be observed. Obviously, the mean level of the thermal noise was already low enough. This must be due to the cooling of the sensor (during the recording sessions) and to the sophisticated read out and signal processing electronics.

2.3.2 Flat field correction

The photo sites of the CCD-sensor vary in sensitivity in a manner similar to random noise. However, the individual photo sites each have fixed sensitivity, so these differences in sensitivity can easily be corrected, eg by recording a picture with a uniform exposure of the CCD-sensor. After dark field subtraction such an image contains variations, which correspond with the actual variations in sensitivity of the photo sites and with the variations in exposure (caused eg by spatial variations in transmission of lens and/or shutter). With the operation given in formula 2.3, a flat field correction can be carried out then.

$$\begin{aligned} Y &= 0 && \text{if } X_{\text{flat}} = 0 \\ Y &= X * (X_{\text{avg}} / X_{\text{flat}}) && \text{if } X_{\text{flat}} > 0 \end{aligned} \quad <2.3>$$

X_{flat} is the individual pixel value in the flat-field image and X_{avg} is the averaged pixel value in the full flat-field image.

Improvements will be observed only if the variations contain high frequency components, because the low spatial frequencies will be suppressed already by the image-processing algorithm. In processing the hereafter mentioned image-database, no significant improvements have been observed with this flat field correction.

2.3.3 Median filtering

This technique can be used to remove the effects of defective pixels within the CCD-sensor. The values of the defective pixels are exchanged by the median of the surrounding pixels. However, this can be done only if the positions of the defective pixels are known.

2.3.4 Histogram modification

The optimum illumination of the sensor with respect to its S/N ratio is an exposure of the sensor up to its saturation level (see chapter four). All the pixel values can be multiplied with a factor up to the maximum value of 4095, in the case when the sensor is underexposed. Processing might give better results then. The effect of exposure is multiplicative. In the future, the histogram of the image-data can possibly be used for an optimum real time exposure of the sensor. In the case when the luminance range of the image is very limited, then better processing results can be obtained by carrying out first a range transformation. Sometimes ,at dense fog, the luminance range is not more than 1 or 2 bit as a result of scattering of light in the atmosphere.

2.3.5 Correction geometrical distortion

The image field is determined only by the focal length of the lens and the dimensions of the sensor (image section). Opaque parts within this image section, as there are the vertical transport CCD-registers in an interline transfer CCD-sensor (see fig.2.4), do not change the field of view. Because of these opaque parts, the number of pixels in both directions is not proportional to the corresponding dimensions of the sensor and a geometrical distortion will appear when the digital data of the image are displayed directly on a monitor. The distance between two adjacent pixels on the monitor is the same in horizontal and vertical direction then.

For the here used Fairchild sensor 222 the horizontal and vertical dimensions are respectively 11.4 and 8.8 mm and the corresponding number of pixels respectively are 380 and 488. Because of these ratios, the image field dimension in the horizontal direction must be multiplied by a factor 1.66.

We have applied only a correction factor of about 1.3, to be able to display 4 pictures on a 1024x1024 screen. The photographs given in chapter 5 have these dimensions therefore.

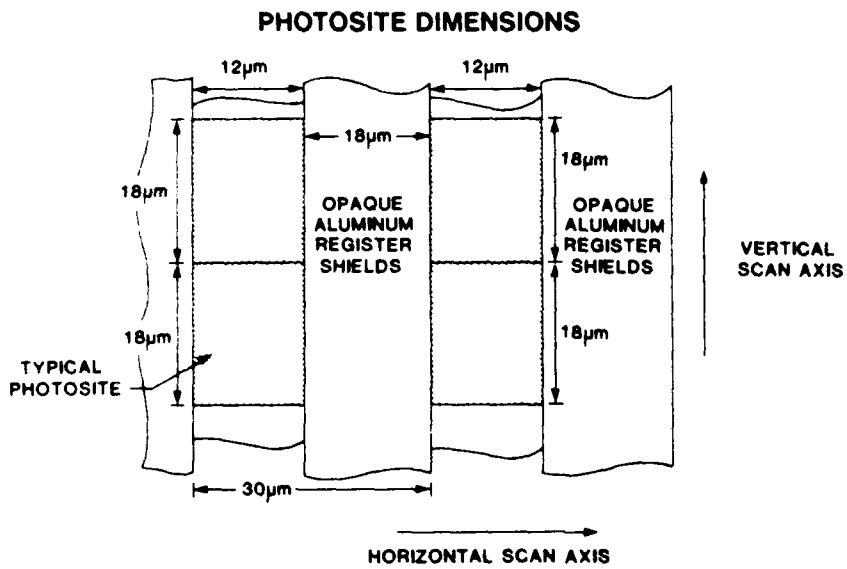


Figure 2.4: Fairchild 222 pixel dimensions (horizontal x vertical = 30 x 18 μm).

3 THE IMAGE DATA BASE

3.1 Introduction

The here described database of images has been set up with the (first) experimental CCD-camera system of the Physics and Electronics Laboratory TNO [1]. An artist's impression of this system is given in fig.3.1. All the pictures have been taken under the various atmospheric conditions occurring in 1988 and 1989. The pictures were all taken from the 11th floor of the FEL tower. This database is mainly used for the evaluation of the described image processing algorithm. The image processing algorithm is extensively described in reference [2] and shortly reviewed in the previous chapter. First the image acquisition will be discussed and then a survey of the available images will be given.

3.2 Image acquisition

All the pictures have been recorded with a CCD-camera system based on the Fairchild CCD 222 sensor. The CCD-sensor is a rectangular array of 384*488 photosites (see figure 2.4). The performance of a 12-bit intrascene dynamic range [1] could be realized by cooling the chip down to -30°C; by compensating the dc-level drift of the video output and by applying special designed analog electronics, like 'correlated double sampling'.

All the pictures have been taken with a 75 mm focal length and a fixed exposure time of 30 mseconds. This was the shortest shutter time to get a nearly homogeneous exposure of the sensor. Part of the images was recorded with a photopic filter (or a 2 mm BG18 glass) in front of the lens to simulate the eye sensitivity. This filter can advantageously be used when the visibility is good, especially in sunlit scenes. Without this filter the near infrared radiation, which is strongly reflected by vegetation, can reduce the local contrasts because of local saturation. Under conditions of limited visibility, due to atmospheric haze, the filter should not be used because of the lower extinction coefficient for the longer wavelengths of near infrared radiation (see chapter 3). For getting an improved S/N ratio, up to 16 images could be added with the modular camera system [1].

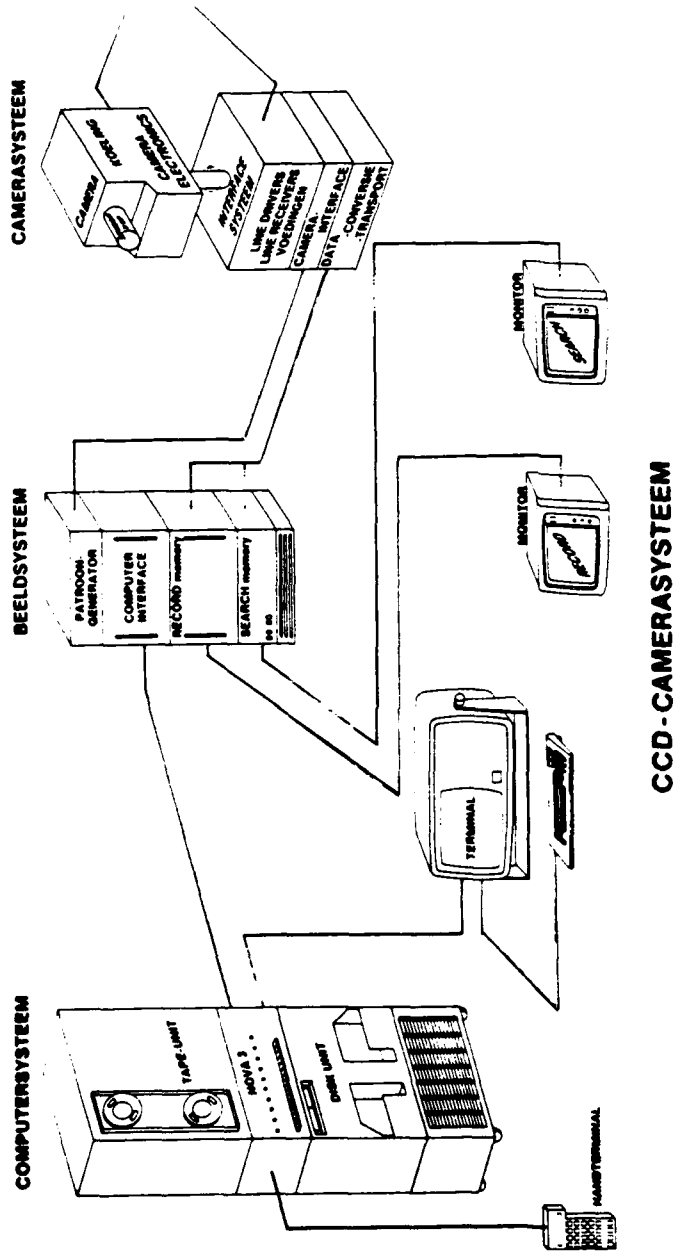


Figure 3.1: Schematic view of the minicomputer controlled LN-cooled CCD camera system and storage equipment.

To get an optimum recording of images, it is important to expose the sensor such that those sensor elements, corresponding with the brightest parts in the scene, are illuminated just till its saturation level. This is because of the Poisson distribution nature of the photon noise, which implies a S/N ratio proportional to \sqrt{n} , n being the number of generated photoelectrons. It results in the best local signal to noise ratio without contrast loss in the brighter parts. Furthermore, the maximum luminance range is recorded then, which is important especially in scenes with a large dynamic range.

3.3 The image database

All the recorded images are pictures taken from the surroundings of the laboratory. The atmospheric conditions, under which the images have been recorded, also have been recorded. With this information, we have been able to relate a number of atmospheric conditions with the parameters of the FEL image processing algorithm. The following meteorological quantities have been noted:

The luminance, the temperature, the relative humidity, the wind speed and wind direction, the cloudiness, the type of weather and of course the visibility.

The visibility is not always unambiguously defined, as will be discussed in chapter 4. The 'eye visibility' of the person (who was always doing the recordings) has been noted together with the visibility measured with an AEG point visibility meter. The location of this PVM, however, was at the seaside boundary of the town near the laboratory, while most of the pictures have been taken in the opposite direction (the 'so called' city views). Furthermore, the range of the visibility that can be reliably measured with such an instrument, is limited from 0.5 to about 15 km.

Recordings have been made for visibilities from 0.1 km up to 30 km. In the scope of a possible application in a military environment, atmospheric conditions with a visibility less than about 5 km are the most interesting. Nevertheless, evaluation of the system for visibilities up to 30 km might also be important because 'facing light' often occurs with good visibility. Figure 3.2 shows a histogram distribution of the recorded images with the corresponding range of the visibility.

Image distribution versus visibility

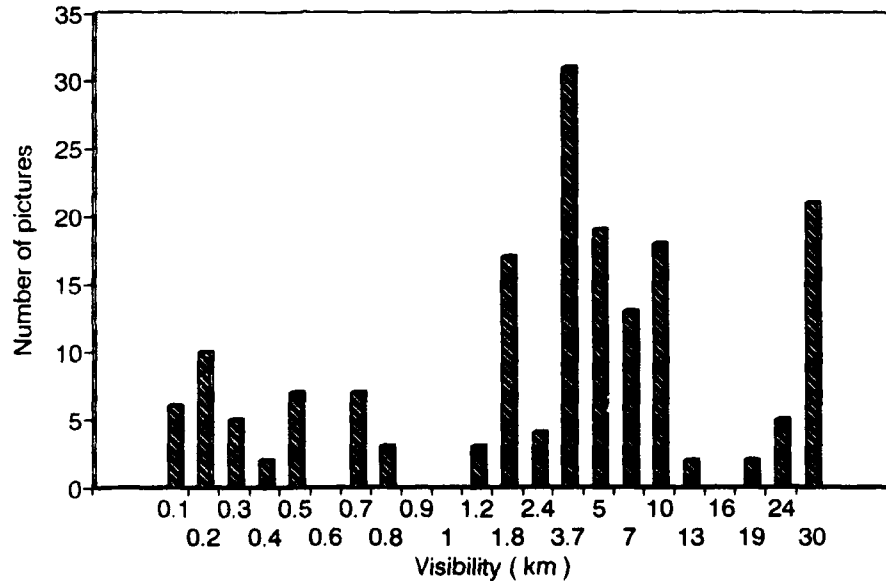


Figure 3.2: Image distribution for the various ranges of the visibility.

In most cases a considerable offset in the greylevel range was present. This might partly be due to the location from which the pictures have been taken. No nearby objects were present, so in most cases this results in a contribution of atmospheric scattering to all parts of the scene. It might also partly be due to scattering at optical parts in the camera head, especially when scenes are recorded with a large luminance range [9,11].

A PC-controlled portable version of the CCD-camera system has been built since then. With this system, pictures can be taken from any location, such that more different scenes can be (and has been) evaluated. In appendix A, a survey is given of all the interesting images, which have been recorded in the here considered period (1988-1989). All these pictures have been processed with the FEL-algorithm to evaluate 12-bit pictures of natural outdoor scenes.

4 VISIBILITY IN THE ATMOSPHERE

The purpose of this chapter is to give a short description of some problems connected with atmospheric properties. One of the goals of this project was to realize a camera system with a visibility range larger than that of commercially available systems. An estimation of the visibility range improvement will be given and an experiment to verify the performance of the camera will be described.

4.1 Theory

Several aspects of the visibility will be discussed briefly. The most important are the optical properties of the atmosphere, the amount and distribution of light, the characteristics of the objects within the field of view and the properties of the human eye. Problems connected with 'visibility' are rather complex. Most of the information, which is acquired through our sense of vision, depends on the perception of differences in luminance and to a lesser extent on chromatics. The contrast (in luminance) in case of an isolated object surrounded by a uniform and rather extended background is given by the equation:

$$C = (L - L') / L' \quad <4.1>$$

L is the luminance of the object and L' is the luminance of the background. The range of C runs from -1 for an ideal black object to ∞ (eg a bright source against a dark background). Due to the extinction of light in the atmosphere [5], the contrast decreases with increasing distance, resulting in a decrease of the visibility. The theory of Koschmieder [5] describes the alteration of contrast due to the path through the atmosphere. For the visual range of an object in the horizontal direction (seen against the horizon sky), the apparent luminance of the object is given by equation 4.2:

$$L = L_0 e^{-\sigma R} + L_h (1 - e^{-\sigma R}) \quad <4.2>$$

Here L_0 is the luminance of the object observed nearby, σ is the extinction coefficient and L_h is the luminance of the horizon. It is assumed that the atmosphere in the horizontal direction is homogeneous. On the same conditions the contrast reduction of the object is given by:

$$C_r = C_0 e^{-\sigma R} \quad <4.3>$$

Now C_0 is the initial contrast of the object (nearby view). The studies of Mie [5] provide a good theoretical basis for the interaction of light and particles in the atmosphere, which determines the extinction coefficient. In case of monodisperse aerosols with no absorption, relation 4.4 is valid:

$$\sigma \approx N \pi a^2 k \quad <4.4>$$

N is the number of particles per cm^3 , a is the radius of the particles and k is the so called scattering area ratio. When the relative humidity for instance is high, the radius of the particles will be large also, in most cases, and the contrast reduction will be large then due to a large extinction and scattering. The extinction coefficient also depends on the wavelength. Various formulas have been proposed and they share the property that σ increases with decreasing wavelength. Rain should be treated as a special case, because the extinction is proportional to the number of drops, falling per unit area per second. Therefore, this parameter should be recorded during the measuring sessions. With increasing distance the contrast will decrease until a certain threshold value is reached at which the object no longer can be seen. Definition of this threshold value might be rather complex. It depends on many parameters and it does not have an unambiguous value. It depends on the properties of the eye, but also on a few nonmeasurable influences, like the physical health, the mental attitude and the alertness of the observer. There are three types of relevant information in the scene: the contrasts, the background luminance and the dimensions of the objects, at which the observer is looking at. Figure 4.1 gives the thresholds related to these parameters. They resulted from experiments, which were organized during the Second World War at the Tiffany Foundation in the United States [5].

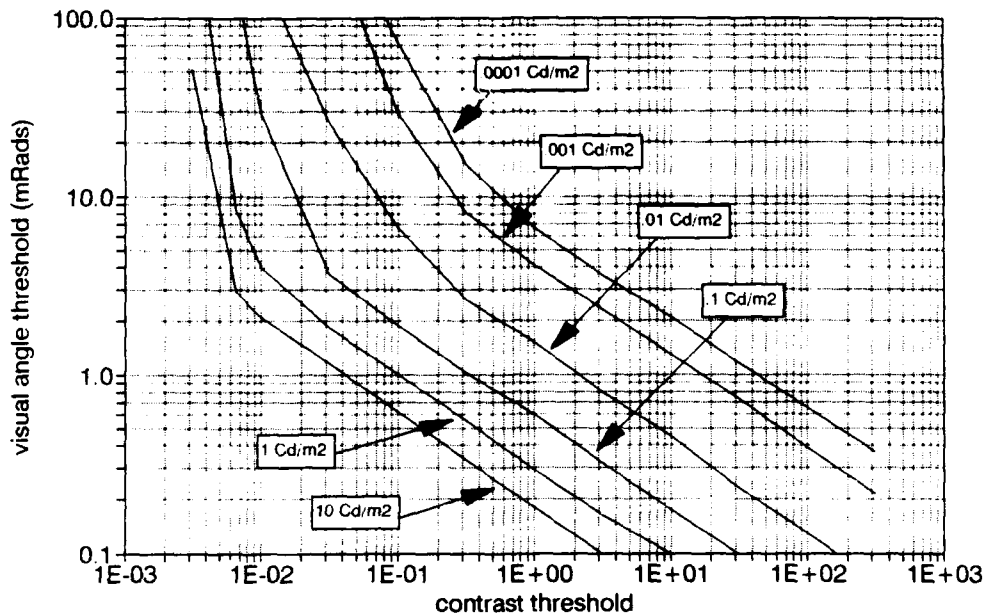


Figure 4.1: Thresholds of brightness-contrast and visual angle (mrads) for 50 percent detection (after Blackwell) at each of the given background luminances. The stimuli were brighter than the background [5].

The threshold dimension of the objects is given by the visual angle in the vertical direction. The contrast thresholds are given only for sources brighter than the background.

It will be clear that it is difficult to define the visual range for a given situation. For most purposes it is accepted to use the so called meteorological visibility, which is defined as the distance along which the transmission due to the atmosphere is decreased to 2%. It is the distance at which an initial contrast $C_0 = 100\%$ is reduced to a contrast $C_r = 2\%$.

It has been mentioned before, that the present investigation is not focussed on the visibility range improvement related to the eye visibility, but to the visibility range of a conventional eight bits TV-perception system. In view of the visibility range improvement, it is useful to know the smallest contrast that can be recorded by the CCD-camera. Although monitor inputs accept eight bit, only about 30 to 60 different grey levels can be distinguished, due to the limited dynamic range of the monitor screen and the human observer. It means that a contrast becomes perceptible, only when a proper contrast enhancement is carried out by the image processing.

When a (threshold) contrast Cr before processing, given by formula 4.3., with $\sigma = \sigma_1$ and $R = R_1$, will increase to Cr' , due to the processing, then this increase can be translated in an apparent decrease of σ to σ_2 . A new apparent visibility range R_2 (with a same final contrast Cr) can be calculated then from this σ_2 . Now formula 4.5 is valid:

$$\sigma_1 R_1 = \sigma_2 R_2 \tag{4.5}$$

With formulas 4.3 and 4.5 a 'visibility range' improvement R_2 / R_1 can be derived with the variables Cr , which is the contrast before processing, Cr' , which is the contrast after processing and Co , being the initial contrast.

$$R_2/R_1 = \frac{\ln(Cr/Co)}{\ln(Cr'/Cr) + \ln(Cr/Co)} \tag{4.6}$$

In figure 4.2 a graph of this 'visibility range' improvement is given as a function of the 'contrast improvement' Cr'/Cr for three values of the 'contrast reduction' factor Cr/Co , due to the atmosphere.

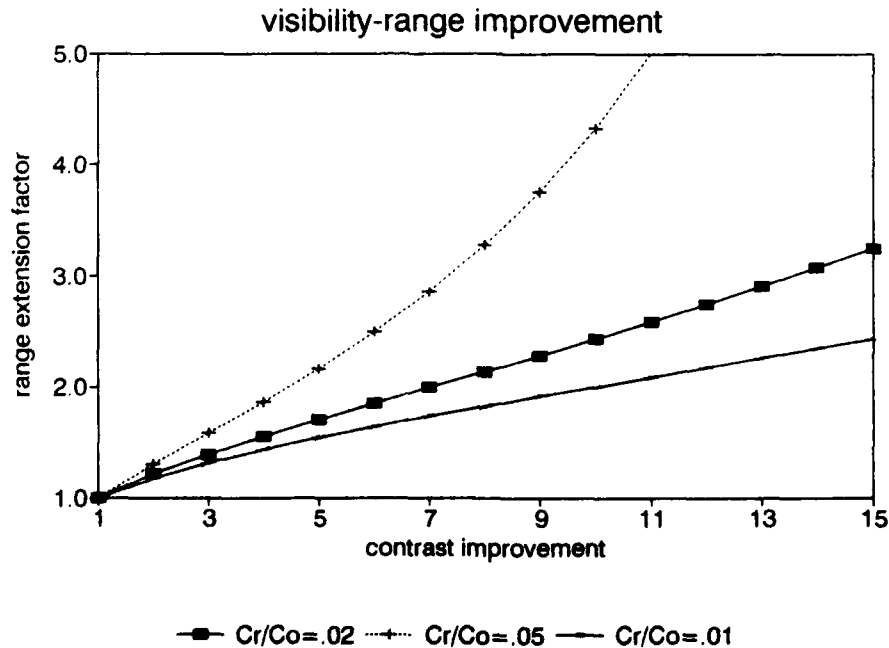


Figure 4.2: The 'visibility range' improvement R_2/R_1 as a function of the 'contrast enhancement' Cr'/Cr for three values of the atmospheric 'contrast reduction' factor Cr/Co .

The maximum contrast enhancement, which can be applied, depends on the signal to noise ratio of the sensor and on the recording conditions. The differences between the three curves indicate the dependence of the 'visibility range improvement' on the perception of the minimum contrast before processing.

To arrive at a reliable validation of the 'visibility range improvement' under adverse atmospheric conditions, an experiment will be necessary, which must be carried out under well defined conditions. Recordings should be made from black and white screens with a known reflection coefficient. These screens must be placed in a straight line at known distances and their dimensions have to increase with increasing distance, such that the viewing angle is the same for all the screens. Variable contrasts of the screens can be realized, eg by projecting black and white lines and lowering their contrasts by an extra screen illumination with a calibrated source. When the screens are selected, which have the same contrasts before and after processing, then a direct 'visibility range improvement' results for the corresponding operational conditions.

Recordings could be made with our 12-bit system and also with an 8-bit system, to evaluate the image processing as function of the camera performance.

5 RESULTS

In this chapter the results of the image processing and the statistical analysis of the image database will be discussed.

5.1 Evaluation of the image processing

It has already been mentioned before, that dark image subtraction did not have a significant effect. Apparently, the applied cooling of the chip down to -30°C has sufficiently lowered the mean level of thermal noise. Also the fixed pattern noise shows to be already low enough and, due to the sophisticated electronics [1], the system noise level as well. A flat field correction was carried out for a few images, but also did not have much effect. Obviously, the sensitivity of the photosites of the used sensor is sufficiently homogeneous. However, in images recorded under conditions of heavy fog, a characteristic vertical oriented pattern becomes perceivable after processing (figure 5.4). This effect may be caused by inhomogeneous illumination, possibly in combination with a digital round off. Due to the limited speed of the shutter blades, the brightness in a recorded image is highest in the middle and is decreasing towards the edges. Every image line is formed by an array of discrete photosites. In the horizontal direction, there is an opaque part of $12\ \mu\text{m}$ between the succeeding sensitive parts of the photosites (see figure 2.4). Then the variation of the brightness along a horizontal image line is not a continuous function. After processing, rectangular areas with different brightness appear. The main spatial frequency in this structure is lower than that corresponding with the pixel pitch. Pre processing, based on histogram modification techniques, gave better results in some cases. When the dc-level of the brightness distribution in the image was valued more than about 2000 (half the saturation level), a better result was obtained by first applying a linear transformation of the recorded grey level range to the full range. Such a high dc-level can arise due to strong backscattering at particles in the atmosphere. In general, the range transformation as given by formula 2.1 is not optimal when only quite small grey level ranges have been recorded. When a linear or a logarithmic range transformation is applied, before the FEL-image processing algorithm is carried out, then a better distribution of the greylevels is obtained.

For a number of images the maximum grey level value was less than 4095. Then it showed to be advantageous for optimum image processing, to multiply first the pixel values such that the maximum value becomes 4095. The best results are acquired by optimizing the exposure during the measuring session such that the maximum pixel value is 4095 in the original picture. Median

filtering can be applied in order to correct defective or hot pixels. Without the mentioned preprocessing methods, the FEL-algorithm still resulted in a significant improvement. Therefore, the preprocessing is not carried out in most of the cases.

After processing, the images need to be transformed according a relation given by <2.1>, to add a gamma correction for a proper monitor display. This is necessary because our CCD-camera is a linear recorder of the scene luminance. In most cases, a gamma of 0.65 was applied with good results. When a larger gamma is used, then the bright part of the image is enhanced at the cost of the dim part and when a smaller gamma is used, the other way around. For a reliable comparison of the original image with the processed image, the original image had to be displayed with a gamma of 0.4, which is a proper gamma correction for most of the monitors. The processing with the FEL-algorithm was carried out with a 3x3 moving average filter, which gave the best results for all the processed images. The parameters γ_d and k_{out} (formula <2.1.>) have been calculated so, that the dynamic range in the output image (without contrast-enhancement) runs from 8 to 224. A sufficient large contrast-enhancement showed to be possible then in all grey level ranges without surpassing the range from 0 to 255 in the final output image. The contrasts have been enhanced till no further improvements could be observed and noise or artefact phenomena started to increase. A value for $\gamma_c=25$ showed to be a good choice for most of the 12-bit images. Exceptions are the scenes with mainly natural vegetation and recorded under bright sky conditions without photopic filter.

For those scenes a $\gamma_c=15$ was a good choice. With the parameter v_n , the contrast enhancement is adapted such that no artefacts will arise. It has been mentioned already in chapter two, that the parameter v_n defines a threshold in the local variance range. Beyond this threshold the contrast enhancement is gradually decreasing to one, according a relationship with v_n as a variable.

It means that with a different v_n , also the adaptation relation will be different. Therefore, some margin in the values of γ_c and v_n will exist, also in case of optimal processing. Artefacts first arise in the pictures at the horizon and they often can be observed in the histogram of the processed image as a peak at greylevel value 255. When the contrasts are strongly enhanced, other artefacts become visible, which are supposed to be related to the array structure of the CCD-sensor. It could be of interest to investigate these artefacts as well as the sources of noise in more detail to determine the limits of a maximum contrast enhancement. It is stressed here once more that the contrasts in the images are affected by the dynamic range reduction due to the transformation from 12 to 8 bit (for presentation purposes on a monitor).

The results obtained with the FEL-algorithm will be discussed now.

This FEL-algorithm gave good results for all the processed images. Images with a dynamic range more than 8 bits, recordings with facing light and scenes with much vegetation were hardly available and should be recorded in the future. It was already mentioned, that a special effect of the shutter might arise in scenes observed through haze. Also the dynamic range transformation showed to be not optimal for images with a very limited grey level range. Due to the structure of the algorithm it is difficult to recognize the effects of the various parameters. The local variance is used to determine the adaptive contrast enhancement; it would be easier to use the local difference in the logarithmic domain, which is equal to the contrast in the input image. The way in which the contrast enhancement is realized for large contrasts depends on the value of v_n and the local variance in the logarithmic domain. Also, this makes it difficult to estimate the effect of v_n , but at the same time it allows some margin in the values of v_n and γ_c . The FEL-algorithm has been compared with wellknown image processing tools like histogram equalizing and histogram stretching. For an image with a large dynamic range (image nr db8910050201, see Appendix A), these processing techniques have been applied to the full image and to a part of the image; in the selected part only a limited grey level range was present. The results are shown in respectively the figures 5.1x for the full image and in the figures 5.2x for the lower right quarter of the same picture. Figure 5.1a gives the original image, without processing; figure 5.1b gives the result of the histogram equalization and figure 5.1c gives the result with the FEL image processing algorithm.

In figure 5.2a the result with histogram stretching is given for the lower right quarter of the same picture as given in figure 5.1. In figure 5.2b the result is given with the FEL image processing algorithm for the same part.



Figure 5.1a: Original 12-bit picture without processing.



Figure 5.1b: Histogram equalization applied to the picture, given in figure 5.1a.

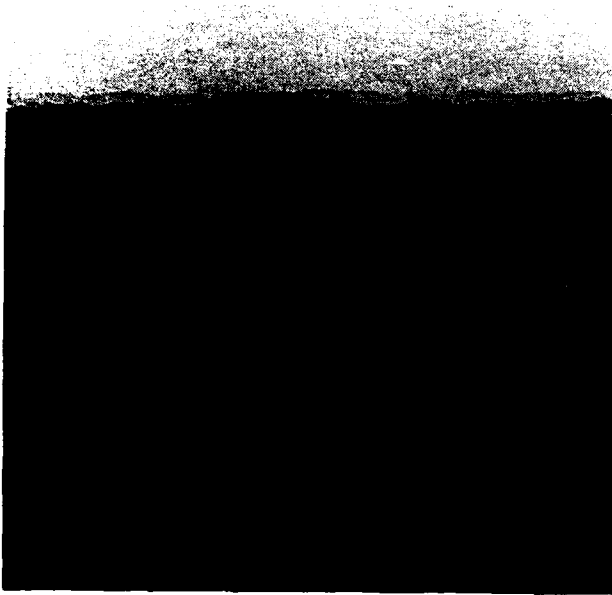


Figure 5.1c: FEL image processing algorithm applied to the picture, given in figure 5.1a.

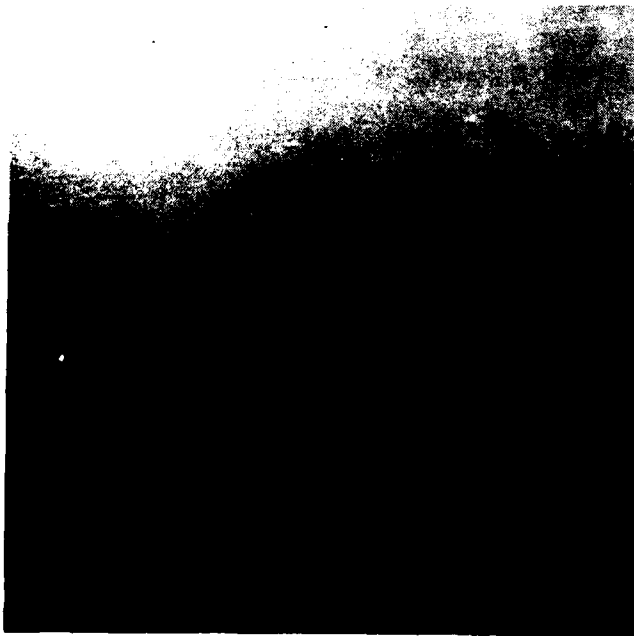


Figure 5.2a: Histogram stretching applied to the lower right quarter of the picture, given in figure 5.1a.

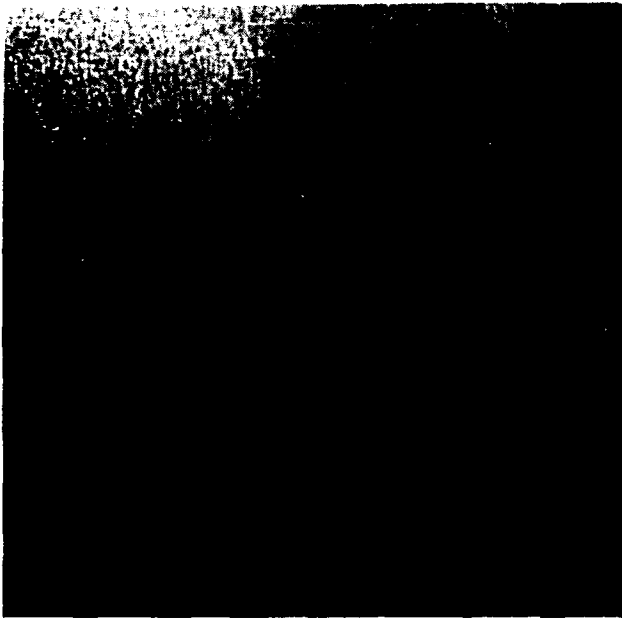


Figure 5.2b: FEL image processing algorithm applied to the lower right quarter of the picture, given in figure 5.1a.

With histogram equalization, a part of the image is enhanced at the cost of another part (see fig. 5.1a and fig. 5.1b). Details in parts with less frequently occurring pixel values can get lost, due to histogram equalization.

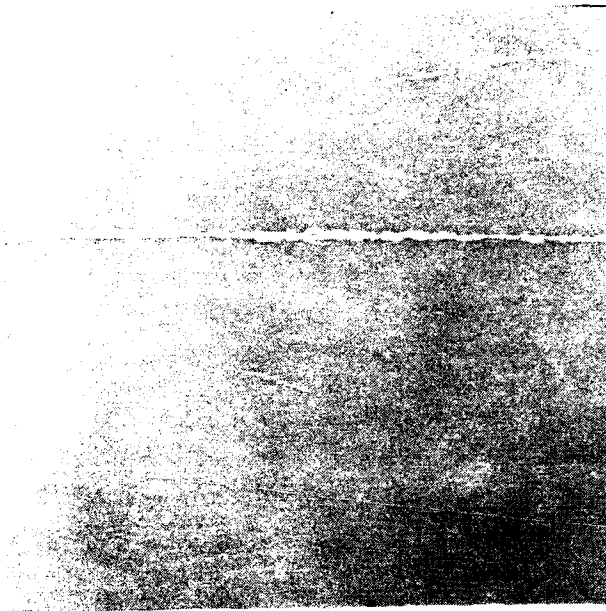
The contrast stretch function can only be used for images with a limited range of succeeding grey values. This also means that there must be no defective photosites causing black or hot pixels or small pixel clusters. The contrast stretch function is not appropriate for detail contrast enhancement. Even when applied to a part of the image only a small improvement can be observed and also now the FEL image processing algorithm results in a much better detailed picture (see fig. 5.2). Comparing figures 5.1c and 5.2b shows that the FEL-algorithm gives already the same result in processing the complete picture as when it is applied to a part of the image, although a larger range is available then for the contrast enhancement (this is to be seen on the monitor, not really good on the photographs). It can be concluded that an algorithm which makes use of local statistics is more suited to enhance an entire image then simple histogram modification techniques.

Because the pictures in figure 5.2. are zoomed in, some of the sensor array structure get to be seen.

Now results with examples will be given for the FEL image processing, applied to images recorded under various atmospheric conditions.

Figure 5.3 shows an image that was recorded with a photopic filter under conditions of heavy atmospheric haze. The visibility varied in the vertical direction from 1.3 to about 4.5 km. Figure 5.4 shows an image recorded at about the same time and with about the same visibility (1.4 to about 4 km), but now recorded without the photopic filter. It can be seen that after processing a significantly better result is obtained, especially in regions in which larger contrasts are expected with near infrared radiation (horizon and regions of vegetation). Without the photopic filter the near infrared radiation contributes to better contrasts in regions of vegetation because of a larger reflection in this spectral region. Also the better transmission of the near infrared wavelengths in dense fog is of importance, especially for the larger distances. In general, a better result is obtained without a photopic filter for visibilities below 8 km, except in sunlit scenes. After processing, small rectangular areas become visible due to the large enhancement. These kinds of artefacts and noise effects are more clearly visible on the monitor. Figure 5.5 shows an image, taken with a photopic filter at a visibility of 7 km. It can be seen that this image should have been recorded without photopic filter. Figure 5.6 shows an image recorded with slight 'facing light' at a visibility of 30 km. It can be seen that the 12-bit camera system, provided with image processing, still can make perceivable more details in this case. Moreover, it results in a sharper picture with a more comfortable vision. Figure 5.7 shows a picture, taken during rain at a visibility of about 10 km. After processing some optical distortions due to the rain become perceivable. Figure 5.8 shows a picture with mainly vegetation, taken with photopic filter at a visibility of about 17 km. It is an example of processing with a lower value for the contrast enhancement parameter ($\gamma_c=15$) in order to prevent artefacts. In scenes with much vegetation, artefacts sooner arise than in the 'city views'. The picture in figure 5.8 gives also a good example of processing, which results in an extended visual range and a remarkable increased comfortable vision. Figure 5.9 finally shows what happens when the photopic filter is not used in a sunlit scene under conditions of good visibility.

5.3a



5.3b



Figure 5.3: Picture taken with photopic filter; visibility from 1.3 to 4.5 km (image dr8811070501, appendix A). Top before and bottom after processing.

5.4a



5.4b

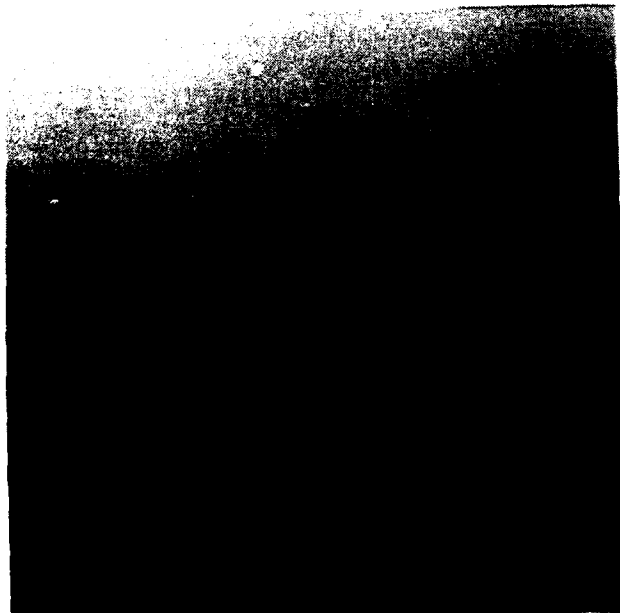


Figure 5.4: Picture taken without photopic filter; visibility from 1.4 to 4km (image dr8811070403, appendix A). Top before and bottom after processing.

5.5a



5.5b

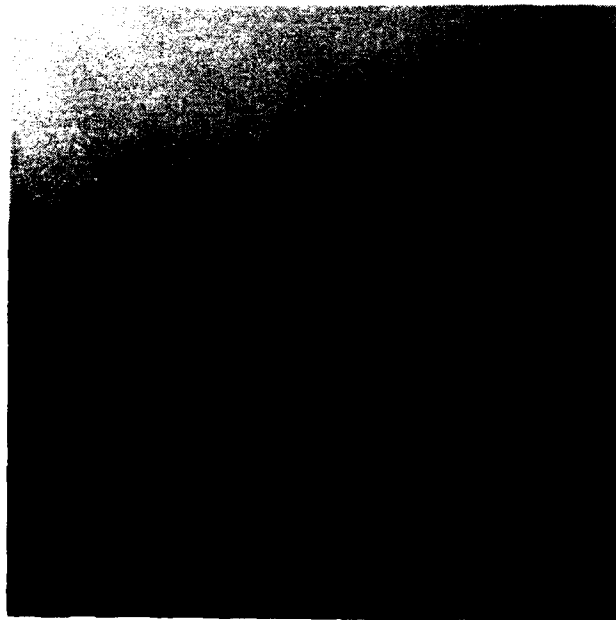


Figure 5.5: Picture taken with photopic filter; visibility 7 km (image m8901270201, appendix A). Top before and bottom after processing.

5.6a



5.6b

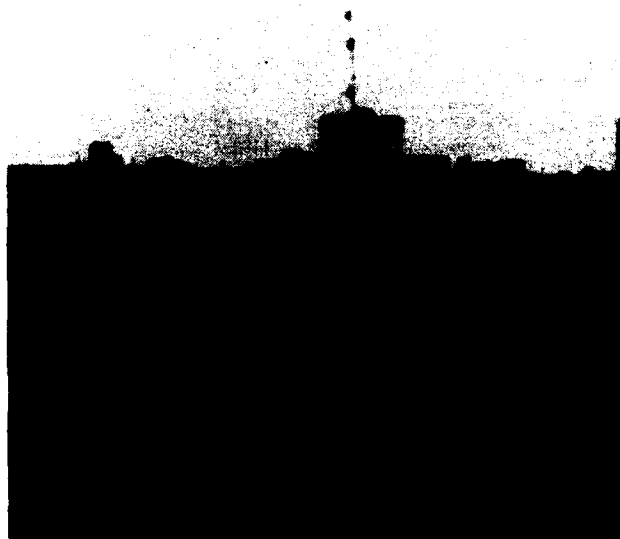


Figure 5.6: Picture taken with photopic filter at a very good visibility of 30 km (image cc8810100601, appendix A). Top before and bottom after processing.

5.7a



5.7b

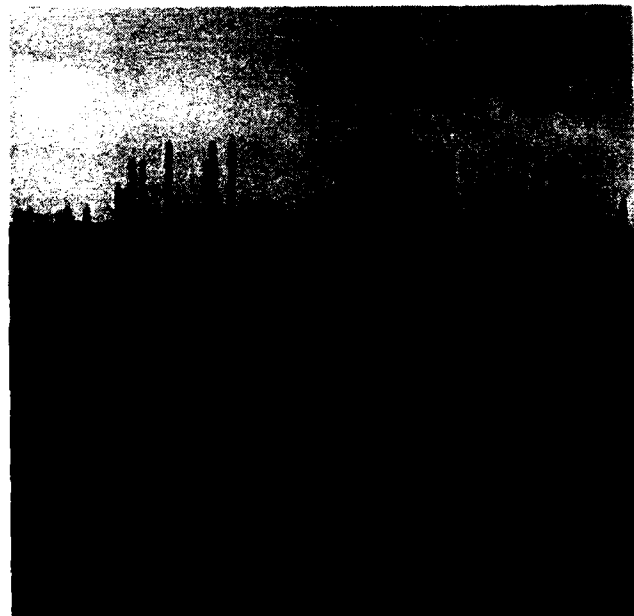
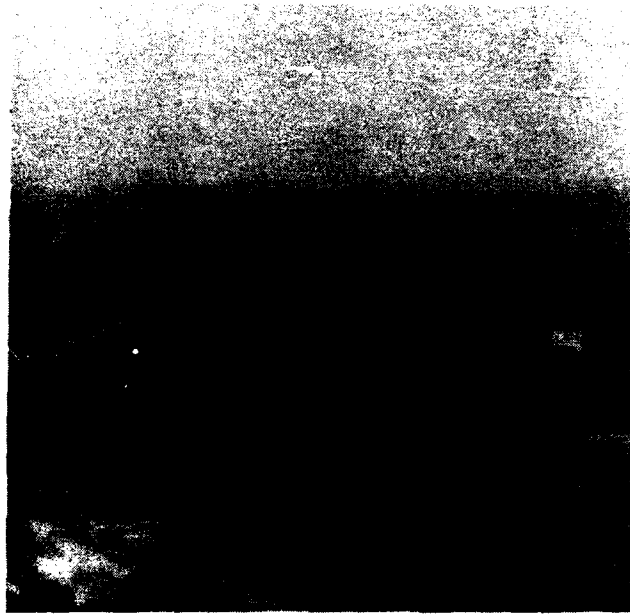


Figure 5.7: Picture taken during rain; visibility 10 km (image st8809230101, appendix A). Top before and bottom after processing.

5.8a



5.8b

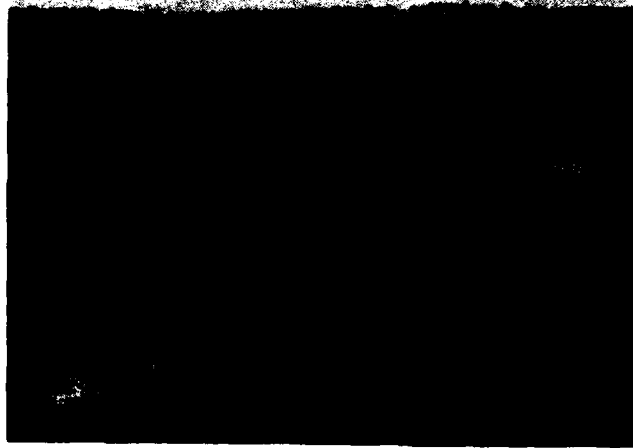


Figure 5.8: Picture with mainly vegetation, taken with photopic filter; visibility 17 km (image dr8811070501, appendix A). Top before and bottom after processing.



Figure 5.9: Unprocessed picture, taken without photopic filter at bright weather; visibility 30 km (image sp8806060103, appendix A).

5.2 Analysis of the image file

Some relations between parameters of the FEL-algorithm and meteorological parameters have been studied, in view of possible automation of the image processing parameters. It has been mentioned before that the parameters γ_d and k_{out} can be calculated from the minimum of the histogram, γ_c can be kept constant (at first instance) and the adaptation parameter v_n can be determined from the calculated local variance. This local variance depends on the atmospheric conditions and the scene. The minimum in the histogram distribution of the grey values depends to a great extent on the scattering of light in the atmosphere (see for the contribution of the background luminance formula 4.2). In general, this minimum value will increase with increasing Relative Humidity and with decreasing Visibility. From studies in the field of atmospheric scattering it is known that the parameter Relative Humidity / Visibility correlates well with atmospheric scattering, especially forward scattering [8].

Some image parameters will be correlated now with the scattering parameter W_{sc} , which therefore is defined as $W_{sc} = \text{Relative Humidity} / \text{Visibility}$.

Figure 5.10 shows the minima of the grey level distributions as a function of this scattering parameter W_{sc} for all the processed images. The given straight line is obtained by a first order linear regression of the logarithmic values of the relevant parameters. A correlation coefficient of about 89% was found. Table 5.1 gives the slopes and interceptions of such regression lines with the correlation coefficients for various selections.

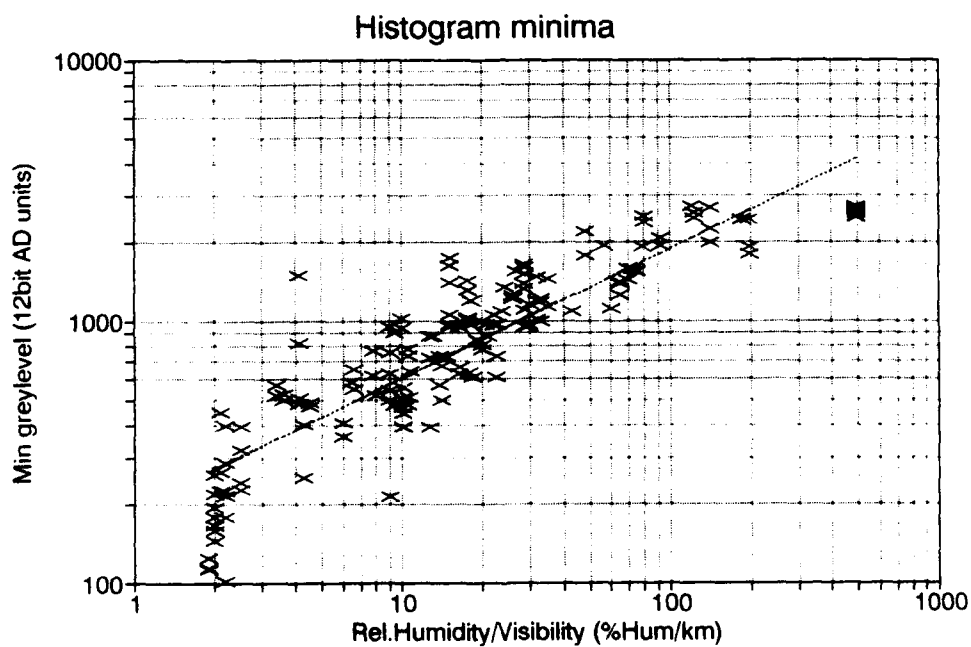


Figure 5.10: Minimum value in the greylevel distributions as function of the scattering parameter W_{sc} for all the processed pictures.

Table 5.1: Relations between atmospheric conditions and some image parameters.

1 nr	2 parameter	3 range	4 filter	5 a	6 b	7 correlation	8 number pict.
1	minimum	0-30	0/1	0.5	2.3	0.89	173
2	..	0-30	0	0.4	2.5	0.89	46
3	..	0-30	1	0.6	2.2	0.9	127
4	..	0-7	0/1	0.4	2.5	0.85	107
5	..	0-7	0	0.3	2.6	0.86	79
6	..	8-30	0/1	0.7	2.1	0.7	66
7	..	8-30	1	0.7	2.1	0.73	50
	loc. var						
8	$v_n/95\%$	0-30	0/1	-1.1	-2.0	-0.79	143
9	$v_n/95\%$	0-30	0	-0.9	-2.0	-0.87	37
10	$v_n/95\%$	0-30	1	-1.2	-1.9	-0.79	110
11	$v_n/chsn.$	0-30	0/1	-0.6	-3.0	-0.57	159
12	$v_n/chsn$	0-30	0/1	-0.7	-3.0	-0.71	88
13	$v_n/chsn$	0-30	1	-0.7	-3.0	-0.72	68
14	$v_n/chsn$	0-30	1	-0.6	-3.0	-0.65	36
15	$v_n/chsn$	0-7	0/1	-0.6	-3.1	-0.54	52
16	$v_n/chsn$	8-30	0/1	-0.8	-2.8	-0.59	36

In table 5.1 the respective columns represent:

1. nr: is the graph number for reference purposes.
2. parameter: is the histogram parameter, which is correlated with the scatter parameter W_{sc} . The local variance parameter $v_n/95\%$ is the value in the local variance histogram distribution at the 95% point. The local variance parameter $v_n/chsn$ is the value of the local variance, which is actually used in the image processing.
3. range: is the visibility range (in km), which is taken into account for the given picture selection.
4. filter: gives the picture selection with respect to the used filter; 0 are pictures taken without filter and 1 pictures taken with a photopic filter.
5. a: gives the slope of the first order regression line with the parameters on a logarithmic scale.
6. b: gives the intersection at the vertical axis (with the histogram parameter) of the first order regression line, the parameters are supposed to be on a logarithmic scale.
7. correlation: correlation coefficient obtained with first order regression.
8. number pict.: number of pictures selected for the respective graphs.

The graph numbers 1 to 7 give the regression line parameters for the graphs with the minimum grey levels in the histogram distributions (graph nr 1 is pictured in figure 5.10); the nrs 8 to 10 give these parameters for the local variance parameter v_n at 95% of its histogram distributions; the nrs 11 to 16 for the local variance parameter v_n , which has been actually used in the processing. The actually used values of v_n at the corresponding percentages in their histogram distributions can be found in column 11 of the list of processed pictures in appendix A.

In graph nr 12 of table 5.1 only the pictures with a contrast multiplier $\gamma_c=25$ are considered. In graph nr 13 only the pictures concerning the city views with a contrast multiplier $\gamma_c=25$ have been taken into account. In graph nr 14 the same pictures as in nr 12 have been considered, but pictures taken with the wind directions west and southwest have been omitted. In the nrs 15 and 16 only the pictures with a contrast multiplier $\gamma_c=25$ have been taken into account.

The visibilities (especially of the 'city views') have been determined by eye, in most cases. This visibility was supposed to be equal to the distance to a relevant reference point, which just could be seen by a trained observer. For visibilities equal to or better than 30 km no such references were available.

The nearest objects in the pictured scenes are at a distance of about 1 km from the camera, which always results in an offset of the grey level range. This offset results from a contribution of light caused by atmospheric scattering (see also formula 4.2). The lowest minimum grey level that has been recorded, amounted to a value 80 (out of 4095 in 12-bit AD units) and the highest about 2800 (see figure 5.10). It might be clear that the dynamic range, in general, depends on the scene itself. In our recordings the maximum grey level value always originated from the sky beyond the horizon and the minimum value from the vegetation on the foreground. The dynamic range parameters γ_d and k_{out} depend on the ratio between the maximum and the minimum luminance, so in our case no explicit dependence on the scene may be expected.

From table 5.1 it can be seen that the correlation with the scatter parameter W_{sc} is better for the minimum greylevel than for the adaptation parameter v_n .

In figure 5.11 the local variance, at the 95% points of the histogram distributions, is given as function of the scatter parameter W_{sc} (Rel.Hum/Vis) for all the processed pictures (graph nr 8 in table 5.1).

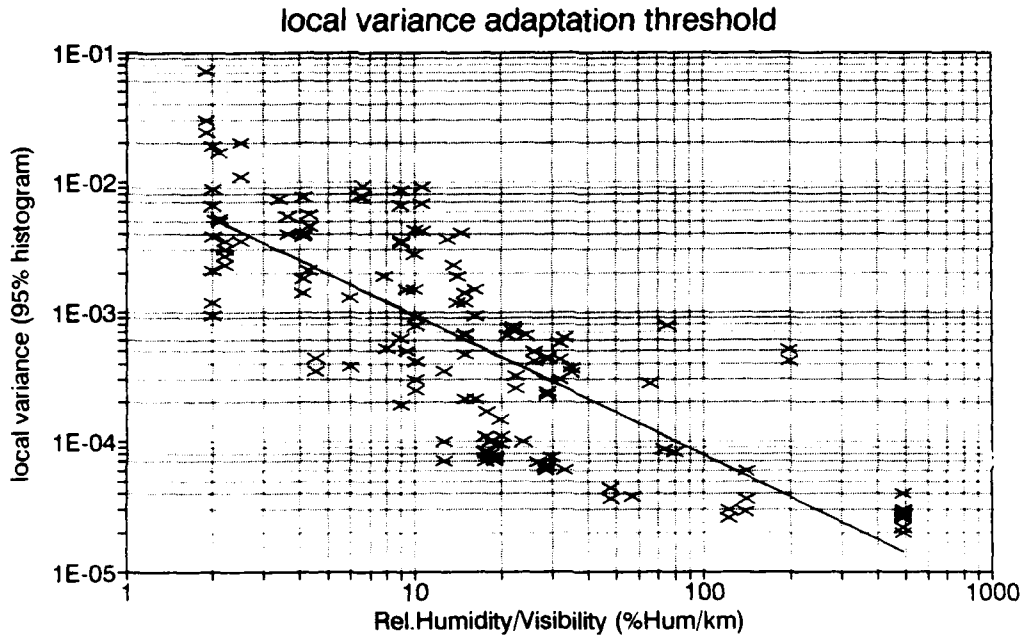


Figure 5.11: Local variance at 95% point of the distributions as function of the scatter parameter W_{sc} for all the processed pictures.

The selections of pictures taken with photopic filter have, in general, a lower value for the intersection parameter 'b' and a steeper slope 'a' than the pictures taken without filter.

The correlation of the adaptation parameter v_n with the scatter parameter W_{sc} is substantially better for a value at a fixed percentage (95%) of its histogram distribution than for the actually used values, which gave (in a subjective sense) the best processing results. The local variance is related to the local contrast, which is determined by the contrasts of the objects in the scene and by the contrast loss in the atmosphere. The scattering increases when the Relative Humidity increases and the Visibility decreases. The parameter $W_{sc} = \text{Relative Humidity} / \text{Visibility}$ therefore is a relevant choice to correlate with. It can be seen from graph 11 in table 5.1 that, when the actually used v_n is related to this scatter parameter W_{sc} for all the images, there is hardly a relevant correlation ($R=0.57$). It must be emphasized here that, when an image is processed with a different γ_c or different dynamic range reduction (output range), the value of v_n will also be different. If only the images with a $\gamma_c=25$ are taken into account and the same dynamic range reduction is applied, then the correlation is better (see figure 5.11, graph nr 12, $R=0.71$).

Because the images are recorded near the coast (North Sea), the scattering aerosol particles are of mainly maritime nature, especially when the wind direction is between south and west. Omitting all the images recorded during such a wind direction, results in a lower correlation coefficient ($R=0.65$), however. This result may be due to the very few points left in this case. Furthermore, there is a fluctuation to expect in the parameter 'chosen v_n ', because the perception of the best processing quality is subjective by nature. The local variance at 95 % of its histogram distributions (see chapter two) gives a better correlation.

It might be concluded that the correlation of the minima in the 'grey level' histogram distributions (and to a lesser extent the parameter v_n) with the scatter parameter W_{sc} is sufficient to use it for a parameter setting of the image processing. However, it seems more reliable to deduce such parameters directly from the histogram distribution of the grey levels, if such histograms are available.

5.3 Visibility range improvement

It was already mentioned in chapter four that it is very hard to determine the visibility range improvement due to image processing. A simple comparison of a monitor presentation of natural scenes before and after the image processing poses special requirements on the composition of the scene. Only a few 12-bit images could be used for this purpose. The distance to only few objects in the scene are known. One must find an object at known distance in the processed image seen against the horizon and a similar object in the original image with about the same contrast. The apparent visibility range improvement due to image processing can be estimated then. For the contrast improvement due to processing, it is necessary to choose an object in the processed image, because an object that becomes perceivable only after processing has the maximum contrast improvement, while the other objects can be processed in an adaptive way. The results for a few images are given in table 5.2. The visibility used in table 5.2 is the visibility estimated by eye during the recordings; R_1 and R_2 are the distances to the objects in respectively the images before processing and after processing; C_r and C_r' the contrasts of the chosen objects in respectively the images before processing and after processing. These contrasts are determined by averaging the grey levels in and around the chosen objects. The 'visibility range improvement' VI can be calculated then with C_r'/C_r from formula 4.6, assuming that $C_o=-1$ (a complete black object according formula 4.1). The dependence of the 'visibility range improvement' on the initial contrast C_o is not analysed.

It can be seen that the 'visibility range improvement' due to the image processing varies from 1.2 to 3.5 for the given examples and premises. The observed visibility (by eye) of course lies in between the distance to the chosen object before processing (R1) and the one after processing (R2).

Table 5.2: Visibility range improvement due to image processing.

filename	visi- bility	R1	R2	R2/R1	C_r	C_r'	C_r'/C_r	VI
st 8809210401	3.4	>1.2	3.4	<2.8	-0.03	-0.08	2.7	1.4
dr 8811090101	4.0	3.4	>4.2	>1.2	-0.02	-0.13	7.0	2.0
dr 8811090102	4.0	3.4	>4.2	>1.2				
db 8907260101	2.5	>1.2	<3.4	<2.8	-0.10	-0.25	2.5	1.7
db 8907260201	4.5	3.4	4.2	>1.2	-0.03	-0.19	6.3	2.1
cc 8810110501	2.7	3.4	>4.2	>1.2	-0.01	-0.04	4.0	1.4
cc 8810110503	3.4	>3.4	>4.2	>1.2	-0.03	-0.16	5.3	1.9
cc 8810110504	3.5	>3.4	>4.2	>1.2	-0.03	-0.17	5.7	2.0
cc 8810110602	4.2	3.4	>4.2	>1.2	-0.01	-0.10	10.0	2.0
dr 8811070601	4.0	1.2	4.2	3.5	-0.01	-0.09	9.0	1.9
dr 8811070501	1.3	1.2	4.2	3.5	-0.02	-0.07	3.5	1.5
dr 8811070703	3.6	3.4	>4.2	>1.2	-0.02	-0.07	3.5	1.5
dr 8811070403	1.4	1.2	4.2	3.5	-0.03	-0.17	5.7	2.0
sp 8810040401	4.0	>1.2	3.5	<2.9	-0.01	-0.04	4.0	1.4
st 8809220201	2.8	0.5	1.2	2.4	-0.03	-0.08	2.7	1.4
st 8809220501	4.5	1.2	4.2	3.5	-0.03	-0.15	5.0	1.8
st 8809220401	3.0	<3.5	>3.5	>1.0	-0.1	-0.18	1.8	1.3
st 8809210101	3.4	1.2	3.4	2.8	-0.04	-0.09	2.3	1.3

The accuracy of the given values is rather low, because often different objects have been compared before and after processing. Nevertheless, they give an indication of what improvement may be expected. In chapter four a better experiment with black and white screens is already proposed. Recordings could already be made from black and white screens with increasing dimensions at increasing distances, for one type of visibility. These screens with an initial contrast $C_0=0.89$ were located at distances of 130, 170 and 290 metres from the camera. The dimensions were such, that in the pictures, the screens all matched with an equal number of pixels on the CCD-sensor. The results are given in table 5.3. The 'visibility range improvement' VI (according formula 4.6), is in the same range as the former estimated improvement from the monitor presentation, notwithstanding the screens were too small to get an accurate contrast value by averaging the grey levels.

Table 5.3: Visibility range improvement from black and white screens.

filename	screen	Cr	Cr'	VI	R2/R1
db8904130101	2	-0.06	-0.3	2.3	>1.7
db8904130203	2	-0.06	-0.3	2.3	2.2
db8904130301	3	-0.06	-0.3	2.3	>1.3

The results from table 5.2. and 5.3. show that the 'visibility range improvement' lies in between 1 and 3. Table 5.3 represents only one weather type: fog with a decreasing density.

5.4 Processing procedure

A straightforward procedure for obtaining optimum processing can be given now for the algorithm, evaluated in this study.

The calculation of the local variance is necessary for the adaptive contrast enhancement. This makes it necessary to store two files, one file containing the local mean and one file containing the local variance of each pixel. The parameter γ_c showed to be rather constant for the here considered kind of scenes (see appendix A: list of processed images and processing parameters). The start values of some parameters may be deduced from the relative humidity/visibility (see the correlation and regression line parameters in table 5.1).

A straight forward procedure now is:

- The range transform parameters γ_d and k_{out} can be determined from the input range (min-max range of the grey level histogram distribution) and the output range (8-224).
- Calculate the local difference file and local variance file with a very low value of v_n (eg 1E-7).
- Take as start value for the adaptation parameter v_n the value at the 95% point in the local variance histogram distribution.
- Lower the value of v_n till all artefacts disappear, while applying a 3x3 window and a maximum value for the contrast multiplier ($\gamma_c=25$).
- Eventually, optimize the value for the contrast multiplier.

6 CONCLUSIONS

- The optimum contrast enhancement factor is rather constant for the considered scenes.
- Extending the database with pictures from other scenes, especially with large dynamic range, is recommended.
- For pictures with a very narrow histogram of the greylevel distribution, the range transformation can better be performed in advance of the local contrast enhancement.
- In case that details in vegetation parts of pictures are important, the use of a photopic filter is necessary at visibilities beyond about 7 km.
- The perception of 'visibility range improvement' by image processing depends among others on the scene, the weather type and the observer. This extension of the visibility range due to processing is expected to lie between 1.5 and 3 times, at least for weather situations with a considerable loss of contrast in the atmosphere.
- It is recommended to quantify the visibility range extension. This may be possible in a special experiment with a large number of well defined targets at different distances. It is important to quantify the usefulness of image processing under various atmospheric and battle field conditions.
- It is recommended to study the positive effects of contrast enhancement on the probability of detection and recognition of military objects.

7 EPILOGUE

Many of the results and insights of the study, described in this report, have been used for demonstrating the power of the image processing algorithm in a number of other CCD-imaging projects.

In order to be able to add pictures from various scenes to the image database, a PC-controlled camera system has been built with a modular, thermo-electric cooled camera head [9,10,11]. A large number of pictures have been taken with this camera system, among others, during the battlefield trial BEST TWO at Mourmelon, France [10].

All the pictures dealt with in this report have been processed on a VAX computer and a I²S image processing station. For most of the interesting applications, a stand alone system with real time processing will be demanded. The processing time with the described algorithm [2], is a serious drawback in eg a PC controlled stand alone station. A general purpose parallel computing system was used for the development of a real time processing system [15]. With four transputers a processing time of about 1 second per frame was realized. Most of the 'Mourmelon' images have been processed with this parallel system [10]. Variations of the algorithm have been studied with real time hardware implementation in mind [12,13]. With fast electronic components a real-time video processor has been realized, which accepts any standard analog video signal [14]. A global range transformation is implemented in this unit directly on the analog video signal with programmable gain and offset. After digitization local adaptive contrast enhancement is carried out.

Finally, within the framework of a national technology project, a 12-bit real time processing system has been developed and realized, together with a number of real time filtering modules [15]. This complete processing system (with filtering and averaging options) is part of a sophisticated EBCCD camera system, but it can accept also any standard analog video signal.

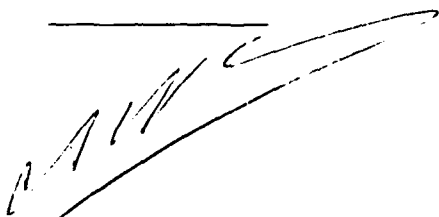
ACKNOWLEDGEMENT

The processing of the images has been carried out by Mr. Ir. J.IJntema. Also he produced most of the statistical results. Therefore, I am very indebted to Mr IJntema for his valuable contributions to this study.

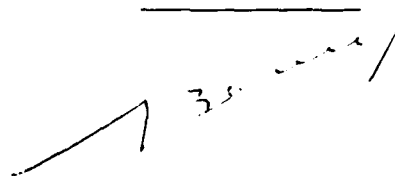
REFERENCES

- [1] Bakker, Ir.T. ea.
De FEL CCD-camera; een experimenteel systeem voor camera-onderzoek en beeldbewerking.
TNO rpt FEL-1987-34.
- [2] Vries, Ir. F.P.Ph de.
Dynamic range reduction and detail contrast enhancement for quality improvement of monitor displayed CCD-images.
TNO rpt. FEL 1988-63.
- [3] Vries, F.P.Ph de.
Automatic, adaptive, brightness independent contrast enhancement
Signal processing 21 (1990) 169-182 .
- [4] Lee, J.S.
Digital image enhancement and noise filtering by use of local statistics.
IEEE Trans. Pattern Anal. Machine Intelligence, Vol. Pami-2, No.2, March 1980, pp165-168.
- [5] Middleton, W.E.K.
Vision through the atmosphere
University of Toronto Press.
- [6] Davidse, Prof. Dr. Ir. D.,
Elektronika B.O.; Elektronische Beeldtechniek cursus 1986, TUD.
- [7] Bosman, Prof.Ir. D.; Ir.F. van der Heijden,
Digitale beeldbewerking
Kollege dictaat, Maart 1988, TUT.
- [8] Boden, Drs J.A,
Forward scattering due to atmospheric aerosol; survey of equipment and typical results for the 1064 nanometer laser wavelength
TNO rpt. FEL 1985-88.
- [9] Boden, Drs J.A.
Een PC-gestuurd 12-bits CCD camerasysteem met Peltier koeling
TNO rpt. FEL-94-..... (to be published).

- [10] Boden, Drs J.A.; M. Deutekom; M.J.Wilmink,
CCD-camera images of BEST-TWO and processing results
TNO rpt. FEL-93-A057.
- [11] Boden, Drs J.A.,
Speciale CCD-systemen
TNO-rpt. FEL 1994-A**, (to be published).
- [12] Lerou, Drs R.J.L.,
Contrastverbetering van video beelden, principes en real-time uitvoeringsaspecten.
TNO-FEL note 8-8-1990.
- [13] Weiden, Ir. A.M. van der,
Comparison of the De Vries and Lerou algorithms with respect to their hardware
implementations.
TNO-FEL note, 1991.
- [14] Coonen, Ir. V.H., e.a.
Real-time video processor to improve hazy video pictures
TNO-FEL data sheet 93/566.
- [15] Zalm, Ir. P.P.M van der, e.a.
NTP-HVCCD eind rapport
HVCCD_P5, september 1993.
company confidential



A.N. de Jong
(group leader)



J.A Boden
(author)

Legend of list of processed recordings.

- 1- filename: abyymmddnncc (eg dr8811030101)
with:
ab=tape / yy=year / mm=month / dd=day / nn=picture nr/ cc=code
code: 01=with photopic filter, 02=id with 8 pictures summed, 03=without filter / 04=id with 8 pictures summed, 05=dark picture.
- 2- lum: Illuminance in kilolux
- 3- zi: Visibility in km
- 4- hu: Relative Humidity in %
- 5- T: Temperature in degrees Celsius
- 6- wo: cloudiness
- 7- wt: weather type
with:
 - 1 = rain
 - 2 = clear with some clouds
 - 3 = sunlit scene
 - 4 = drizzle
 - 5 = fog
 - 6 = fog, decreasing density
 - 7 = haze at some distance
 - 8 = some local cloudiness
 - 9 = haze
 - 10 = decreasing haze
 - 11 = clear
 - 12 = dark weather
- 8- γ_d : exponent of range transformation
- 9- k: constant in range transformation
- 10- γ_c : contrast multiplier in logarithmic domain
- 11- $v_n/\%$: local variance in logarithmic domain for the given % in its histogram distribution; this value has actually been used in the processing.
- 12- min: lowest grey level value
- 13- $v_n/95$: local variance in logarithmic domain for the 95% point in its histogram distribution.
- 14- S: description of the scenes
with:
 - 1 cityview 1 with Bronovo hospital
 - 2 cityview 2 with barrack building
 - 3 cityview 3 with central station
 - 4 cityview 4 with Esso building
 - 5 white house between dunes/woods
 - 6 small building in dunes near TNO-FEL parking
 - 7 read roof / a-hove
 - 8 parking STC
 - 9 roof STC

15- opm: remarks

with:

- 1 = visibility measured by AEG point visibility meter near TNO-FEL laboratory
- 2 = not used in the statistics
- 3 = bad part in picture
- 4 = white vegetation due to omission of photopic filter
- 5 = application of NIR passing filter RG695
- 6 = no information perceivable after processing
- 7 = not standard output window (which is 8,224)
- 8 = grey level scaling before processing
- 9 = no homogeneous visibility in vertical picture direction
- 10 = facing light present in picture
- 11 = 7*7 filter window applied in local contrast enhancement (standard is 3*3)
- 12 = complete picture below the horizon

Appendix A: List of processed images and processing parameters

filenaam	lum KL	zi Km	hu z	T	w o	w t	γ_d	k	γ_c	vn/%	min	vn/95	S	opm
rn8812020304	1.4	0.2	99	-2	8	5	7.53	4.13e-25	40	2e-5/95	2280	2.2e-5	2	-
rn8812020402	1.4	0.2	99	-2	8	5	7.80	1.63e-26	?	?	2650	2.7e-5	2	-
rn8812020603	1.2	0.2	99	-2	8	5	8.17	2.87e-27	25	2e-5/95	2296	2.0e-5	1	-
rn8812020501	1.2	0.2	99	-2	8	5	8.02	2.81e-27	25	3e-5/95	2650	3.0e-5	1	-
cc8810110101	5.3	0.2	99	5	8	5	7.09	5.33e-24	25	3e-5/95	2560	2.8e-5	2	6
cc8810110103	3.1	0.2	99		8		1.00	5.47e-20	25	0.1	2489	-		2/6
st8809220101	-	0.2	99	10	8	5	7.09	5.33e-24	?	?	2560	2.9e-5	1	6
rn8812020101	2.1	0.2	99	-2	8	5	6.80	6.40e-23	35	4e-5/95	2480	4.0e-5	2	-
rn8812020203	1.4	0.2	99	-2	8	5	7.60	2.26e-25	50	3e-5/95	2280	2.6e-5	2	-
rn8901240103	1.0	0.5	92	0	8	5	1.24	7.00e-3	10	1e-3/85	2172	-	8	8
rn8901240201	1.0	0.5	92	0	8	5	1.24	6.50e-3	10	9e-4/87	2449	-	8	8
rn8902090303	33	0.5	99	0	4	5	4.05	5.21e-13	35	7e-5/85	1799	4.2e-4	9	-
rn8902090401	22	0.5	99	0	4	5	4.42	2.41e-14	30	6e-5/85	1927	5.1e-4	9	-
db8904130703	5.5	0.5	98	5	8	5	1.00	5.00e-2	10	5e-2/-	2120	-	-	2/8
rn8902090501	44	0.7	99	0	4	5	5.56	1.90e-18	25	4e-5/95	2248	5.6e-5	2	-
rn8902090603	66	0.7	99	1	3	5	4.58	8.62e-15	25	6e-5/95	1847	6.0e-5	2	-
sp8810040201	22	0.7	98	12	7	?	7.98	3.38e-27	20	2e-5/85	2697	2.9e-5	2	-
sp8810040202	28	0.8	98	12	7	9	7.25	1.72e-24	20	2e-5/90	2535	2.6e-5	2	-
sp8810040101	7	0.8	98	12	7	9	6.52	6.12e-22	25	2e-5/85	2457	3.0e-5	2	-
sp8810030101	18	0.8	96	10	8	6	8.38	1.16e-28	20	6e-5/99	2752	-	2	-
rn8901240301	0.9	1.0	92	0	8	5	1.27	6.00e-3	10	5e-4/85	1940	-	8	8
rn8901240403	0.9	1.0	92	0	8	5	1.24	7.00e-3	10	9e-4/75	1940	-	8	8
cc8810110203	7	1.2	95	5	8	10	4.42	4.23e-14	25	8e-5/95	1700	8.3e-5	2	-
sp8810030201	28	1.2	96	10	8	6	6.73	1.09e-22	20	7e-5/99	2496	-	2	-
sp8810030301	28	1.2	96	10	8	6	6.15	1.42e-20	15	2e-5/85	2381	-	2	-
cc8810110201	7	1.3	95	5	7	10	3.48	6.23e-11	25	9e-5/95	1570	8.7e-5	2	-
dr8810140103	22	1.3	98	9	4	6	3.43	1.40e-10	25	6e-5/5	1375	7.8e-4	2	1
dr8811070501	16	1.3	98	2	4	6	3.40	1.19e-10	25	1e-4/70	1536	-	1	9
dr8811070403	5.5	1.4	98	2	2	5	3.18	7.57e-10	30	1e-3/60	1434	-	1	9
dr8811070301	7.5	1.4	98	2	2	5	3.52	4.49e-11	25	1e-5/70	1587	-	2	9
dr8811070203	5.5	1.5	98	2	2	5	3.19	7.45e-10	25	2e-4/63	1408	-	2	9
dr8810140201	28	1.5	98	10	4	6	3.08	1.62e-9	25	3e-5/50	1390	2.8e-4	2	1
sp8810040301	44	1.5	85	15	4	9	4.47	1.60e-14	25	4e-5/95	1943	3.8e-5	2	-
dr8810140301	44	1.5	97	10	4	10	2.82	1.51e-8	20	2e-4/72	1254	-	1	1
dr8810140403	44	1.6	97	10	4	10	2.55	1.71e-7	20	1e-4/45	1024	-	1	1
sp8810030401	30	2.0	96	10	7	6	5.36	9.48e-18	25	4e-5/95	2200	3.6e-5	2	-
sp8810030501	33	2.0	96	10	7	6	4.0	8.00e-13	20	4e-5/95	1780	4.4e-5	2	-
dr8810140501	45	2.2	95	10	4	10	2.51	1.86e-7	20	2e-4/68	1088	-	1	1
db8907260101	22	2.5	80	21	8	-	2.39	1.96e-6	25	2e-5/-	583	5.7e-4	1	-
st8809210402	40	2.6	62	19	3	9	2.51	1.96e-7	25	1e-4/95	1065	1.0e-4	1	-
sp8810030701	6.7	2.7	89	14	8	9	2.67	5.19e-8	25	3e-5/75	1174	6.1e-5	2	-
sp8810030702	5.5	2.7	89	14	8	9	2.74	2.73e-8	25	5e-3/94	1216	-	2	-
cc8810110303	22	2.7	95	9	7	10	3.19	7.83e-10	25	4e-4/95	1360	3.7e-4	2	-
cc8810110402	19	2.7	95	9	8	5	2.63	7.11e-8	25	3e-4/95	1140	3.4e-4	2	-
filenaam	lum KL	zi Km	hu z	T	w o	w t	γ_d	k	γ_c	vn/%	min	vn/95	S	opm

Appendix A: List of processed images and processing parameters

filenaam	lum KL	zi Km	hu z	T	w o	w t	γ_d	k	γ_c	vn/z	min	vn/95	S	opm
cc8810110501	19	2.7	90	9	7	10	2.36	6.49e-7	25	6e-4/95	1000	6.3e-4	1	-
st8809220201	57	2.8	80	15	7	6	2.96	4.70e-9	25	7e-5/95	1326	6.6e-5	1	-
st8809220202	57	2.8	80	15	8	6	3.08	1.80e-9	25	6e-5/95	1342	6.1e-5	1	-
st8809220301	66	2.8	80	15	7	6	3.65	1.45e-11	25	6e-5/95	1635	6.4e-5	2	-
st8809220302	66	3.0	80	15	7	6	3.43	1.00e-10	25	7e-5/95	1500	6.9e-5	2	-
dr8810060603	66	3.0	90	10	3	9	2.68	4.93e-8	20	1e-4/40	1152	-	1	1
sp8810030601	5.5	3.0	89	15	8	9	2.29	1.21e-6	20	8e-5/95	955	7.5e-5	1	-
sp8810030602	5.5	3.0	89	15	7	9	2.30	1.13e-6	35	1e-5/95	960	-	1	-
dr8810140603	66	3.0	90	10	3	9	2.68	4.93e-8	20	1e-4/40	1152	?	1	-
cc8810110302	18	3.0	95	9	8	5	3.27	4.16e-10	25	3e-4/95	1400	3.0e-4	2	-
cc8810110301	22	3.0	95	9	8	5	2.71	3.50e-8	25	4e-4/95	1200	4.3e-4	2	-
cc8810110503	11	3.4	90	9	7	10	2.75	2.72e-8	25	5e-4/95	1210	4.9e-4	1	-
st8809160101	-	3.4	43	13	8	4	2.15	3.80e-6	25	1e-4/95	870	1.0e-4	2	-
st8809160102	-	3.4	43	13	8	4	1.92	2.60e-5	25	7e-5/95	722	7.0e-5	2	-
st8809160201	-	3.4	43	13	8	1	1.42	2.65e-3	25	1e-4/70	284	3.5e-4	2	-
cc8810120103	3.1	3.4	98	9	2	6	3.55	3.48e-11	35	2e-4/85	1600	4.5e-4	1	-
cc8810120101	2.8	3.4	98	9	2	6	2.28	1.30e-6	25	8e-5/85	950	2.4e-4	1	-
cc8810120201	2.8	3.4	98	9	2	10	2.54	1.56e-7	25	1e-4/85	1100	2.3e-4	2	-
cc8810120203	2.8	3.4	98	9	2	10	3.34	2.00e-10	35	2e-4/85	1510	4.3e-4	2	-
st8809210101	44	3.4	60	17	4	9	2.39	5.50e-7	25	1e-4/95	990	1.1e-4	1	-
st8809210102	44	3.4	60	17	4	9	2.42	4.20e-7	25	8e-5/95	1031	8.4e-5	1	-
st8809210201	44	3.4	60	17	4	9	3.15	1.00e-9	20	6e-5/90	1420	8.2e-5	2	-
st8809210202	44	3.4	60	17	4	9	2.92	6.60e-9	?	?	1306	7.0e-5	2	-
st8809210302	40	3.4	62	19	3	9	2.71	5.40e-8	25	8e-5/95	1042	8.0e-5	2	-
st8809210301	40	3.4	62	19	3	9	2.71	3.50e-8	25	8e-5/95	1200	8.0e-5	2	-
st8809210401	40	3.4	62	19	3	9	2.32	9.70e-7	25	1e-4/95	971	1.0e-4	1	-
cc8810110504	11	3.5	90	9	7	10	2.80	1.74e-8	25	4e-4/95	1228	4.2e-4	1	-
dr8811070703	88	3.6	82	8	3	9	2.32	9.40e-7	20	2e-4/60	973	-	1	-
st8809220401	88	3.7	83	18	7	9	1.94	2.20e-5	25	3e-4/95	735	3.2e-4	2	-
st8809220402	88	3.7	83	18	7	9	1.75	1.06e-4	25	3e-4/95	609	2.6e-4	1	-
st8809270201	1.4	4.0	-	17	8	12	1.54	5.94e-4	25	2e-4/95	473	1.5e-4	2	-
dr8811070601	73	4.0	82	8	3	9	2.32	9.40e-7	25	2e-4/75	973	-	1	-
dr8811090101	2.8	4.0	88	8	8	9	2.30	1.18e-6	25	2e-4/80	935	7.7e-4	1	-
dr8811090102	3.4	4.0	88	8	8	9	2.46	3.21e-7	25	2e-4/85	1021	7.1e-4	1	-
cc8810120303	3	4.0	97	9	2	10	2.98	3.80e-9	35	3e-4/85	1340	6.7e-4	1	-
sp8810040401	66	4.0	80	13	4	9	2.06	8.36e-6	30	8e-4/90	810	1.1e-4	2	-
cc8810110802	14	4.2	90	9	8	10	2.15	3.80e-6	25	1e-4/80	870	6.5e-4	2	-
sp8810040402	44	4.2	80	13	6	9	2.12	4.95e-6	30	7e-5/95	850	7.2e-5	2	-
st8809220601	7	4.2	83	18	8	9	2.36	6.50e-7	25	7e-7/90	1000	9.6e-5	1	-
sp8810040501	44	4.5	80	13	6	9	1.79	7.60e-5	25	1e-4/90	637	1.7e-4	1	-
db8907260201	30	4.5	65	21	1	9	1.94	2.29e-5	25	1e-4/80	732	4.1e-3	1	1
st8809220501	75	4.5	83	18	7	9	1.75	1.07e-4	15	4e-4/-	610	-	1	-
db8907260301	33	5.0	65	21	1	9	2.15	3.8e-6	25	?	870	3.6e-3	2	-
filenaam	lum KL	zi Km	hu z	T	w o	w t	γ_d	k	γ_c	vn/z	min	vn/95	S	opm

Appendix A: List of processed images and processing parameters

filenaam	lum KL	zi Km	hu z	T	w o	w t	γd	k	γc	vn/z	min	vn/95	S	opm
sp8810060101	1.4	6.0	98	11	8	1	1.78	8.30e-5	20	1e-4/90	630	2.1e-4	1	-
sp8810060201	1.4	6.0	98	11	8	1	1.84	5.02e-5	25	2e-4/70	670	9.3e-4	1	-
sp8810060203	1.0	6.0	98	12	8	1	2.28	1.29e-6	20	4e-4/80	950	1.5e-3	1	-
sp8804070101	9.0	6.0	90	12	-	9	3.10	2.80e-9	20	6e-3/85	1124	1.4e-3	5	1
sp8804070102	9.0	6.0	90	12	-	9	3.60	4.39e-11	20	5e-4/85	1344	1.2e-3	5	1
sp8804070103	9.0	6.0	90	12	-	9	3.88	1.06e-11	20	2e-4/85	1156	4.7e-4	5	1
sp8804070201	9.0	6.0	90	12	-	9	2.27	1.60e-6	25	2e-4/85	883	6.8e-4	4	1
sp8804070202	9.0	6.0	90	12	-	9	2.46	3.59e-7	25	2e-4/85	960	6.7e-4	4	1
sp8804070203	9.0	6.0	90	12	-	9	2.31	1.13e-6	30	2e-5/60	910	2.1e-4	4	1
cc8810110603	2.8	6.0	82	11	8	4	1.93	2.35e-5	25	5e-4/80	730	2.3e-3	1	-
cc8810110601	7.5	6.0	82	11	8	4	1.69	1.76e-4	25	1e-4/60	570	2.3e-3	1	-
rn8901270101	66	7.0	74	7	5	9	1.27	5.80e-3	20	4e-4/82	512	-	1	7
rn8901270201	66	7.0	74	7	5	9	1.57	4.50e-4	25	5e-4/85	512	-	1	7
rn8901270403	66	7.0	75	7	5	9	1.42	1.60e-3	25	1e-2/80	640	-	2	7
rn8901270303	66	7.0	74	7	5	9	1.57	4.50e-4	25	3e-4/70	512	-	1	7
rn8901270501	52	7.0	75	8	5	9	1.42	1.60e-3	25	3e-4/81	640	-	2	7
rn8901270601	52	7.0	75	8	5	9	1.42	1.60e-3	25	5e-4/81	640	-	2	7
sp8810060303	1.0	7.0	98	12	8	1	1.85	4.70e-5	20	7e-4/85	675	1.9e-3	2	-
sp8810060301	1.0	7.0	98	12	8	2	1.59	4.23e-4	20	4e-4/85	500	1.2e-3	2	-
st8809160401	19	8.0	81	15	8		1.54	6.67e-4	25	4e-4/95	450	4.1e-4	2	-
st8809160402	19	8.0	81	15	8		1.59	4.21e-4	25	4e-4/95	490	4.2e-4	2	-
st8809160301	22	8.0	81	15	8	9	1.51	8.30e-4	25	3e-4/95	441	3.0e-4	2	-
st8809160302	22	8.0	81	15	8	9	1.67	2.10e-4	25	3e-4/95	557	2.5e-4	2	-
st8809160501	22	8.0	81	15	8	9	1.43	1.62e-3	25	1e-4/65	390	7.8e-4	1	-
st8809160502	22	8.0	81	15	8	9	1.42	1.71e-3	25	1e-4/70	383	9.2e-4	1	-
st8809270101	2.1	8.0	-	17	8	12	1.62	3.09e-4	25	2e-4/95	525	1.6e-4	1	-
dr8810130101	44	8.0	84	11	6	7	1.55	5.44e-4	25	4e-4/50	480	6.8e-3	1	1
dr8810130103	44	8.0	84	11	6	7	2.01	1.23e-5	25	4e-4/50	780	4.2e-3	1	1
dr8810130201	70	8.0	84	11	6	7	1.95	2.06e-5	25	1e-4/30	740	9.2e-3	2	1
dr8810130303	66	8.0	80	12	6	7	2.40	4.70e-7	25	2e-4/35	1023	4.3e-3	2	1
dr8810130304	66	8.0	80	12	6	7	2.28	1.34e-6	25	2e-4/55	940	1.5e-3	2	1
dr8810130402	66	8.0	80	12	6	7	1.59	4.10e-4	25	3e-4/50	491	2.8e-3	2	1
db8910050301	77	10	80	18	1	11	1.62	3.29e-4	25	1e-2/?	520	5.2e-4	7	10
db8910050501	14	10	66	16	0	11	1.81	6.46e-5	15	2e-3/70	650	9.3e-3	7	-
db8910050701	14	10	66	16	0	11	1.66	2.35e-4	25	2e-4/25	547	7.7e-3	7	-
db8910050901	11	10	65	17	0	-	1.70	1.59e-4	25	5e-4/40	578	7.8e-3	7	-
st8809230101	5.5	10	90	14	8	1	1.45	1.40e-3	25	2e-4/95	400	1.9e-4	1	-
st8809230201	5.5	10	90	14	8	1	1.13	1.87e-2	25	6e-4/95	214	6.2e-4	1	-
sp8806080101	1.4	10	90	16	-	6	1.65	2.59e-4	25	2e-4/40	520	8.8e-3	3	1
sp8806080102	1.4	10	90	16	-	6	1.78	8.84e-5	25	2e-4/45	606	6.6e-3	3	1
sp8806080103	1.4	10	90	16	-	6	2.28	1.77e-6	?	?	830	3.4e-3	3	1
sp8806080107	1.4	10	90	16	-	6	1.97	2.59e-5	?	?	613	3.5e-3	3	1
dr8811110203	1.0	10	94	13	-	12	2.20	2.55e-6	25	2e-4/70	900	1.5e-3	2	1
filenaam	lum KL	zi Km	hu z	T	w o	w t	γd	k	γc	vn/z	min	vn/95	S	opm

Appendix A: List of processed images and processing parameters

filenaam	lum KL	zi Km	hu Z	T	w o	w t	γ_d	k	γ_c	vn/Z	min	vn/95	S	opm
dr8811110301	0.6	10	94	13	8	12	1.55	5.79e-4	25	1e-4/70	475	5.0e-4	2	1
dr8811110101	1.0	12	94	13	8	12	1.77	9.42e-5	25	1e-4/50	620	1.9e-3	1	1
dr8811110103	1.0	12	94	13	8	12	1.99	1.40e-5	25	1e-4/50	770	1.9e-3	1	1
st8809230301	4.2	15	90	14	7	1	1.45	1.35e-3	25	4e-4/95	408	3.8e-4	2	-
st8809230302	88	15	90	14	7	1	1.37	2.59e-3	25	1e-3/95	347	1.3e-3	2	-
st8804270101	-	17	70	14	-	3	2.08	6.88e-6	15	1e-3/70	825	7.7e-3	5	1
st8804270103	-	17	70	14	-	3	3.32	5.00e-10	10	5e-6/10	1150	1.8e-3	5	1
st8804270201	-	17	70	14	-	3	1.56	5.80e-4	25	9e-4/80	450	4.0e-3	4	1
st8804270202	-	17	70	14	-	3	1.60	4.24e-4	?	?	470	3.8e-3	4	1
st8804270203	-	17	70	14	-	3	1.59	4.00e-4	25	6e-4/85	501	1.4e-3	4	1
db8910050101	77	18	81	17	1	2	1.54	6.17e-4	25	4e-4/95	470	3.5e-4	7	10
db8910050201	77	18	81	17	1	2	1.56	5.04e-4	25	4e-4/95	486	4.4e-4	7	10
db8909290103	-	20	85	13	7	-	1.44	1.44e-3	25	2e-3/?	400	2.1e-3	7	-
db8909290201	5k5	20	85	13	7	-	1.20	1.08e-2	15	3e-3/90	252	4.6e-3	7	-
db8909290301	5k5	20	85	13	7	-	1.20	1.06e-2	15	2e-3/75	253	5.7e-3	7	-
dr8811040101	11	24	86	-2	0	2	1.62	3.05e-4	25	4e-4/70	526	4.0e-3	1	1
dr8811040203	19	24	86	-2	0	2	1.58	4.23e-4	10	1e-3/60	500	5.5e-3	1	1
dr8811040303	22	25	84	-1	0	2	1.61	3.30e-4	10	8e-4/60	520	7.4e-3	2	1
dr8811040401	29	25	84	-1	0	2	1.69	1.76e-4	20	4e-4/50	570	7.4e-3	2	1
st8809290101	58	29	65	14	5	3	1.43	1.50e-3	25	6e-4/70	400	3.0e-3	2	1
st8809290201	15	29	65	14	5	2	1.13	1.82e-2	25	7e-4/85	216	2.3e-3	2	1
st8809290401	88	29	65	14	5	2	1.26	6.54e-3	25	4e-4/60	289	3.5e-3	1	1
st8809290402	22	29	65	14	5	2	1.06	3.28e-2	25	6e-4/80	175	2.3e-3	1	1
st8809290202	14	29	65	14	5	2	1.15	1.65e-2	25	1e-3/90	220	2.3e-3	2	1
st8809290501	19	29	65	14	5	2	0.90	1.23e-1	25	5e-4/70	102	2.7e-3	1	1
sp8809290201	88	29	85	14	5	2	0.82	2.54e-1	25	2e-2/-	80	-	2	-
cc8810100103	16	29	60	12	2	2	1.51	8.00e-4	15	4e-4/50	450	5.2e-3	2	-
cc8810100203	22	29	60	12	2	2	1.22	9.00e-3	20	1e-3/80	265	5.0e-3	1	-
cc8810100301	22	29	60	12	2	2	1.15	1.60e-2	20	1e-3/50	225	1.7e-2	1	-
cc8810100401	88	29	58	13	3	2	1.14	1.70e-2	35	2e-4/50	220	6.6e-3	1	-
sp8806060101	8	30	75	13	-	8	1.15	1.70e-2	25	4e-4/30	209	2.0e-2	3	1
sp8806060102	8	30	75	13	-	8	1.18	1.37e-2	25	3e-4/30	223	1.1e-2	3	1
sp8806060103	8	30	75	13	-	8	1.31	4.40e-3	25	1e-4/80	307	3.5e-3	3	4
sp8806060107	8	30	75	13	-	8	1.42	2.45e-3	25	2e-5/20	321	3.5e-3	3	5
rn8902230301	44	30	58	6	1	2	0.92	1.05e-1	20	1e-3/10	51	7.2e-2	6	1
cc8810100603	44	30	60	13	2	2	1.02	4.50e-2	30	4e-4/80	158	9.5e-4	2	6
cc8810100601	33	30	60	13	2	2	1.07	3.15e-2	25	5e-4/60	180	3.8e-3	2	6
cc8810100602	22	30	60	13	2	2	1.09	2.50e-2	30	6e-4/80	195	2.1e-3	2	6
cc8810100501	88	30	60	13	2	2	1.00	5.60e-2	35	2e-4/40	145	8.9e-3	1	6
cc8810100503	88	30	60	13	2	2	1.21	9.60e-3	30	5e-4/85	260	1.2e-3	1	6
cc8810100101	16	30	60	11	2	2	1.03	4.00e-2	20	7e-4/50	167	1.9e-2	2	-
filenaam	lum KL	zi Km	hu Z	T	w o	w t	γ_d	k	γ_c	vn/Z	min	vn/95	S	opm

REPORT DOCUMENTATION PAGE

(MOD-NL)

1. DEFENSE REPORT NUMBER (MOD-NL) TD93-3418	2. RECIPIENT'S ACCESSION NUMBER	3. PERFORMING ORGANIZATION REPORT NUMBER FEL-93-A323
--	---------------------------------	---

4. PROJECT/TASK/WORK UNIT NO. 22270	5. CONTRACT NUMBER A90KL675	6. REPORT DATE FEBRUARY 1994
--	--------------------------------	---------------------------------

7. NUMBER OF PAGES 53 (INCL. 1 APPENDIX, EXCL. RDP AND DISTRIBUTION LIST)	8. NUMBER OF REFERENCES 15	9. TYPE OF REPORT AND DATES COVERED
---	-------------------------------	-------------------------------------

10. TITLE AND SUBTITLE
EVALUATION OF FEL IMAGE PROCESING ALGORITHM FOR 12-BIT CCD-IMAGES AS FUNCTION OF VARIOUS ATMOSPHERIC CONDITIONS

11. AUTHOR(S)
J.A. BODEN

12. PERFORMING ORGANIZATION NAME(S) AND ADDRESS(ES)
TNO PHYSICS AND ELECTRONICS LABORATORY, P.O. BOX 96864, 2509 JG THE HAGUE
OUDE WAALSLOORPERWEG 63, THE HAGUE, THE NETHERLANDS

13. SPONSORING/MONITORING AGENCY NAME(S)
ROYAL NETHERLANDS ARMY
VAN DER BURCHLAAN 31, 2597 PC THE HAGUE, THE NETHERLANDS

14. SUPPLEMENTARY NOTES
THE CLASSIFICATION DESIGNATION ONGERUBRICEERD IS EQUIVALENT TO UNCLASSIFIED.

15. ABSTRACT (MAXIMUM 200 WORDS, 1044 POSITIONS)
A SURVEY IS GIVEN OF PROCESSING RESULTS OF 12-BIT PICTURES WITH THE FEL IMAGE PROCESSING ALGORITHM. THE RESULTS ARE ILLUSTRATED WITH EXAMPLES. THE PICTURES HAVE BEEN TAKEN WITH THE FIRST FEL 12-BIT CCD CAMERA SYSTEM UNDER VARIOUS ATMOSPHERIC CONDITIONS. SOME RELATIONS BETWEEN PROCESSING PARAMETERS AND ATMOSPHERIC CONDITIONS ARE ANALYSED. AN INDICATION OF A QUANTITATIVE VISIBILITY RANGE IMPROVEMENT IS GIVEN.

16. DESCRIPTORS ATMOSPHERIC PROPAGATION CONTRAST SIGNAL PROCESSING	IDENTIFIERS VISUAL IMAGING VISIBILITY RANGE EXTENSION IMAGE PROCESSING CCD CAMERA PERFORMANCE STATISTICAL RESULTS
---	--

17a. SECURITY CLASSIFICATION (OF REPORT) ONGERUBRICEERD	17b. SECURITY CLASSIFICATION (OF PAGE) ONGERUBRICEERD	17c. SECURITY CLASSIFICATION (OF ABSTRACT) ONGERUBRICEERD
---	---	---

18. DISTRIBUTION/AVAILABILITY STATEMENT UNLIMITED	17d. SECURITY CLASSIFICATION (OF TITLES) ONGERUBRICEERD
--	---